Molecular Therapy
Nucleic Acids
Original Article

circFLT1 and lncCCPG1 Sponges miR-93 to Regulate the Proliferation and Differentiation of Adipocytes by Promoting lncSLC30A9 Expression

Zihong Kang,[1] Sihuang Zhang,[1] Enhui Jiang,[1] Xinyu Wang,[1] Zhen Wang,[1] Hong Chen,[1] and Xianyong Lan[1]

[1]College of Animal Science and Technology, Northwest A&F University, Yangling Shaanxi 712100, China

Although many circular RNAs (circRNAs) and long non-coding RNAs (lncRNAs) have been discovered in adipocytes, their precise functions and molecular mechanisms remain poorly understood. Based on existing circRNA and lncRNA sequencing data of bovine adipocytes, we screened for the differential expression of *circFLT1* and *lncCCPG1* in preadipocytes and adipocytes and further analyzed their function and regulation during adipogenesis. The overexpression of *circFLT1* and *lncCCPG1* together facilitated adipocyte differentiation and suppressed proliferation. Computationally, the RNA hybrid showed that *circFLT1* and *lncCCPG1* had multiple potential binding sites with miR-93. Additionally, luciferase reporting experiments verified that *circFLT1* and *lncCCPG1* may interact with miR-93. We also demonstrated that overexpressed miR-93 effectively suppresses the expression of *lncSLC30A9*. Signaling pathway enrichment analysis, luciferase activity assay, and expression analysis revealed that *lncSLC30A9* inhibits proliferation by inhibiting the expression of AKT protein and promotes differentiation by recruiting the FOS protein to the promoter of peroxisome proliferator-activated receptor gamma (*PPARG*). In sum, our results elucidate the regulatory mechanisms of *circFLT1* and *lncCCPG1* as miR-93 sponges in bovine adipocytes.

INTRODUCTION

Qinchuan cattle are among the best local cattle breeds in China. The breed has the advantages of tall stature, strong bones, well-developed muscles, and favorable meat production performance. Generally, the main evaluation indexes of beef quality include marbling, juiciness, tenderness, color, and texture of fat as well as flavor, water content, and pH. Most of these indexes are related to the growth and development of adipose tissue. Therefore, research on beef fat, especially on the molecular mechanisms of bovine adipocyte proliferation, apoptosis, and differentiation, is crucial to bovine breeding in China.

Adipose tissue is an important tissue, as it can be used for energy storage and supply and can participate in physiological and pathological regulation. Adipose tissue is mainly composed of adipose stem cells (precursor cells to generate new fat cells) and adipose cells (fat storage cells). Their main function is to maintain the energy balance in the body by storing triglycerides and facilitating fat mobilization.[1,2]

Adipogenesis is generally divided into two stages. The first stage is the differentiation of embryonic stem cells into mesenchymal stem cells with multi-differentiation potential. The second stage is terminal differentiation, whereby the preadipocytes have the characteristics of mature adipocytes and acquire lipid droplets and the ability to respond to hormones, such as insulin.[3] These phases are associated with the processes of adipocyte apoptosis, differentiation, and proliferation, which are regulated by a series of transcription factors and adipokines and lead to adipocyte development.[4,5]

Much progress has been made in the study of genetic polymorphism and the function of adipogenesis genes. In the field of non-coding RNA, microRNAs (miRNAs) are known to play important regulatory roles in adipogenesis. For example, miR-204 facilitates adipocyte differentiation by targeting *Sirt1*,[5,6] and miR-93 can regulate adipocyte differentiation by inhibiting *Sirtuin-7* and *T-box3*.[7]

lncRNA regulation of adipogenesis has also attracted increasing attention at the transcriptional, epigenetic, and post-transcriptional levels. The lncRNA *ADNCR* promotes *Sirt1* gene expression through adsorption of miR-204 and thereby inhibits adipocyte differentiation.[5] The lncRNA *IMFNCR* promotes the expression of the promoter of adipogenic differentiation-related gene (*PPARG*) through adsorption of miR-128-3p and miR-27b-3p, thereby promoting adipocyte differentiation[8].

The role of circRNA in the regulation of fat development and its mechanisms remains unclear. In light of previous studies of miRNAs and lncRNAs and the lack of research on circRNAs, this study aimed to analyze the molecular mechanisms of circRNA and lncRNA adsorption of miRNA to regulate adipogenesis and define the regulatory network of bovine fat development. Early screening high-throughput sequencing was used to evaluate Qinchuan cattle fat cells at different periods of differentiation and their associated lncRNAs and circRNAs. Key lncRNAs and circRNAs are known to be involved in the generation and regulation of fat cells in Qinchuan cattle.

Received 22 May 2020; accepted 11 September 2020;
https://doi.org/10.1016/j.omtn.2020.09.011.

Correspondence: Xianyong Lan, PhD, College of Animal Science and Technology, Northwest A&F University, Yangling, Shaanxi 712100, China.
E-mail: lanxianyong79@126.com

However, further study is required to determine the mechanisms of proliferation and differentiation. At the non-coding RNA level, we aimed to characterize the regulation of fat development and the origin of excellent meat quality traits in Qinchuan cattle. The use of non-coding RNA as a molecular marker in Chinese beef cattle breeds may provide a new theoretical basis for the selection of superior genetic traits.

RESULTS

Identification of miR-93 in Bovine Adipocytes

Laboratory data for Qinchuan cattle, including adipocyte differentiation on days 0, 6, and 9; the results of cell transcriptome sequencing; and random screening of differentially expressed miRNAs revealed an association between adipose differentiation and the differential expression of six miRNAs. The real-time qPCR results were basically consistent with the results of sequencing (Figure S1). We selected adipocytes with the highest levels of expression of miR-93 and the most significant differences in the expression of miR-93 for further analysis to explore the role of miR-93 in fat development (Figure 1A).

Primary bovine fat cells were isolated for induced differentiation. Successful differentiation was verified by detecting the expression level of differentiation marker genes and Oil Red O staining (Figures 1B–1E). We then detected changes in the expression of miR-93 during differentiation (days 0, 2, 4, 6, 8, and 10). The trend in expression was consistent with that observed in sequencing, with the highest expression level at day 6 of differentiation (Figure 1F). Similarity analysis indicated that the miR-93 seed sequence was conserved among cows, mice, and humans (Figure 1G). Thus, we speculate that miR-93 might be a potential regulator during adipogenesis.

Effects of miR-93 on Adipocyte Proliferation, Apoptosis, and Differentiation

To determine whether miR-93 regulates adipocyte proliferation and apoptosis, we conducted the 5-ethynyl-20-deoxyuridine (EdU) assay, flow cytometry, cell counting kit-8 (CCK-8) assay, real-time-PCR, and western blotting. Detection of overexpression efficiency showed that miR-93 expression was markedly increased (Figure 2A). We used the EdU incorporation assay to detect cell proliferation and observed that miR-93 promoted the mitotic activity of adipocytes (Figure 2B). Flow cytometry demonstrated that the number of S phase cells was increased upon miR-93 overexpression (Figure 2C). Subsequently, CCK-8 detection produced similar findings (Figure 2D). In addition, we observed that the proliferation-related markers, including cyclinD, cyclinE, and proliferating cell nuclear antigen (PCNA) expression levels were significantly increased following the overexpression of miR-93 (Figures 2E and 2F). Further assay detection showed that miR-93 significantly increased both mRNA and protein expression levels of Bcl-2 (Figures 2G and 2H). Conversely, knockdown of miR-93 inhibited cell proliferation and promoted cell apoptosis (Figures S2A–S2G). These results indicate that miR-93 stimulates proliferation and suppresses apoptosis. To further explore the involvement of miR-93 in adipocyte differentiation, changes in its expression at days 0, 2, 4, 6, 8, and 10 of differentiation were detected. The results showed that miR-93 expression was first increased and then reduced, and its highest expression occurred on day 6 of differentiation (Figure 1B). Detection of overexpression efficiency showed that miR-93 expression was markedly increased (Figure 2I). After transfection with pcDNA3.1-miR-93 or pcDNA3.1, the mRNA and protein expression levels of the adipose differentiation markers PPARG, CEBPA, and FABP4 were also decreased on day 6 of differentiation (Figures 2J and 2K). Fewer lipid droplets were detected in the pcDNA3.1-miR-93-transfected adipocytes via Oil Red O staining on day 6 of differentiation (Figure 2L). Interference with miR-93 promoted cell differentiation (Figures S2H–S2K). Collectively, these results indicate that miR-93 suppresses adipocyte differentiation. Given that miR-93 is highly conserved among cows, mice, and humans, we also assessed its function in 3T3-L1 cells. The overexpression of miR-93 promoted 3T3-L1 cell proliferation and inhibited 3T3-L1 cell differentiation (Figure S3). These findings relating to 3T3-L1 cells are consistent with our bovine adipocyte findings.

LncSLC30A9 Is a Target lncRNA of miR-93

To explore the molecular mechanism by which miR-93 regulates adipogenesis, we used the bioinformatics software TargetScan and considered three candidate genes associated with adipogenesis. The luciferase reporter assay showed that when the psi-Sirt7-3′UTR or psi-SLC30A9-3′UTR wild type was co-transfected with pcDNA-miR-93, the luciferase activity was significantly reduced. No significant change was noted in luciferase activity in the co-transfected mutant vector group (mutation seed region −3∼−6 site). However, luciferase activity was significantly decreased when psi-PDGFRA-3′UTR wild type or psi-PDGFRA-3′UTR mutant type was co-transfected with pcDNA-miR-93 (Figure 3A). This observation may stem from the fact that the mutations were unsuccessful, suggesting that *PDGFRA* may be a target gene of miR-93.

As several studies have now clarified the effects of *Sirt7* on fat function, we focused on the effects of *SLC30A9* on fat function.[7] We found that the *SLC30A9* 3′ end could produce two lncRNAs, which were differentially expressed both before and after differentiation.[5] The rapid amplification of cDNA ends (RACE) analysis of adipocytes showed that *lncSLC30A9* had two transcripts, named *lncSLC30A9a* and *lncSLC30A9b*, which were 1296 nt and 848 nt in length, respectively (Figures 3B and 3c).

The bioinformatics software, Coding Potential Calculator (CPC), was used to evaluate the coding potential. *lncSLC30A9* had a very low coding potential, which was similar to that of another bovine non-coding RNA, *MEG9* (Figure 3D). We then overexpressed miR-93 and detected a significant reduction in *lncSLC30A9* mRNA expression in bovine adipocytes (Figure 3E).

However, we detected no significant differences in miR-93 expression among *lncSLC30A9*-overexpressed cells (Figure 3F). To confirm the binding between *lncSLC30A9* and miR-93, we performed dual-luciferase assays, which showed that luciferase activity in the *lncSLC30A9* wild type was reduced (Figure 3G). The results of luciferase activity at different doses further demonstrated the relationship between

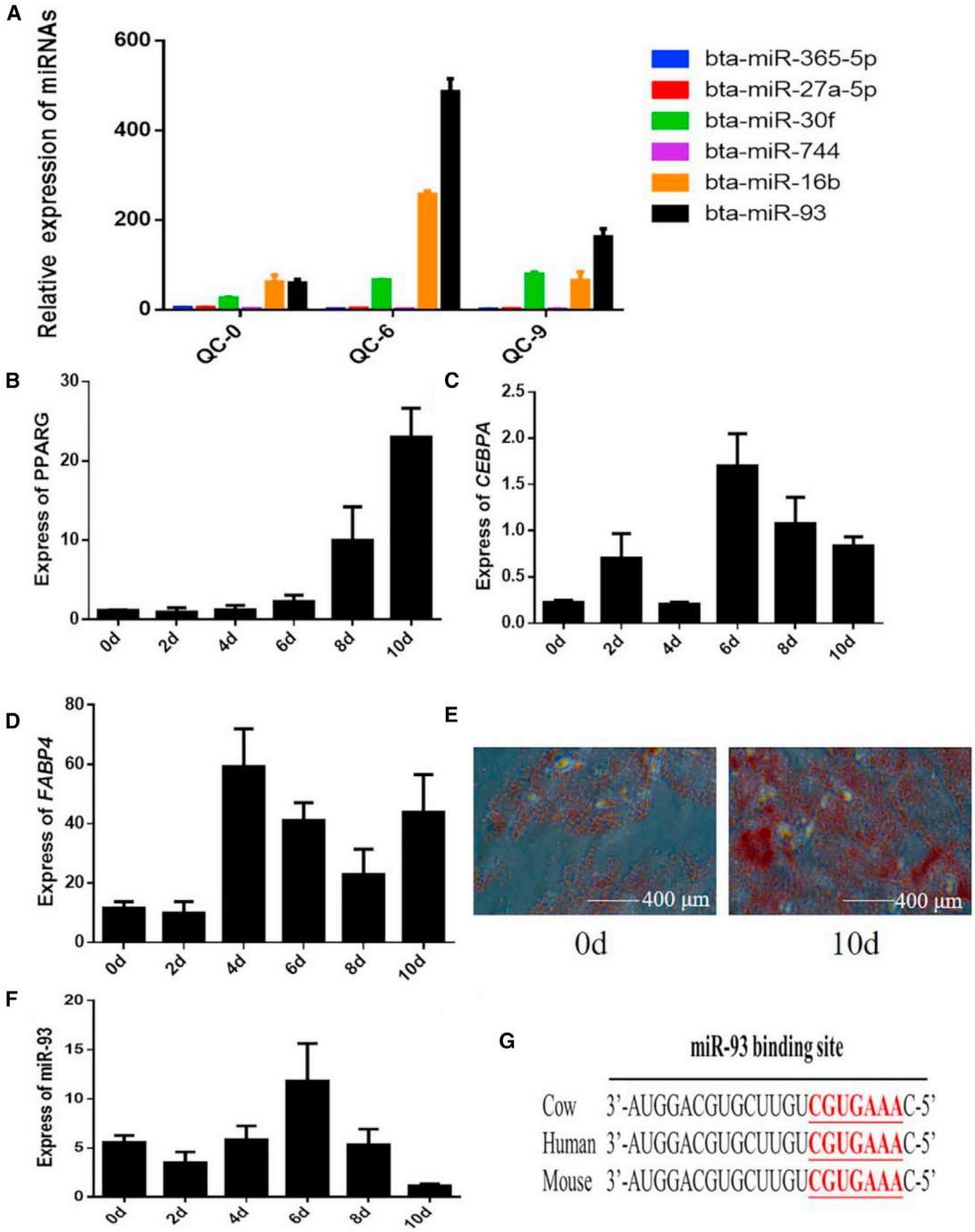

Figure 1. The Expression of miR-93 in Bovine Adipocytes

(A) Expression of six miRNAs in adipocytes of Qinchuan cattle. QC-0, QC-6, and QC-9 represents induction of adipocyte differentiation in Qinchuan cattle for 0 days, 6 days, 9 days, respectively. (B–E) The mRNA expression of marker genes *PPARG* (B), *CEBPA* (C), *FABP4* (D) at different stages of differentiation and Oil Red O staining (E). (F) Expression of miR-93 in Qinchuan cattle adipocytes at different stages of differentiation. (G) The similarity analysis of miR-93 in cow, human, and mouse. Values are mean ± SEM for three biological replicates.

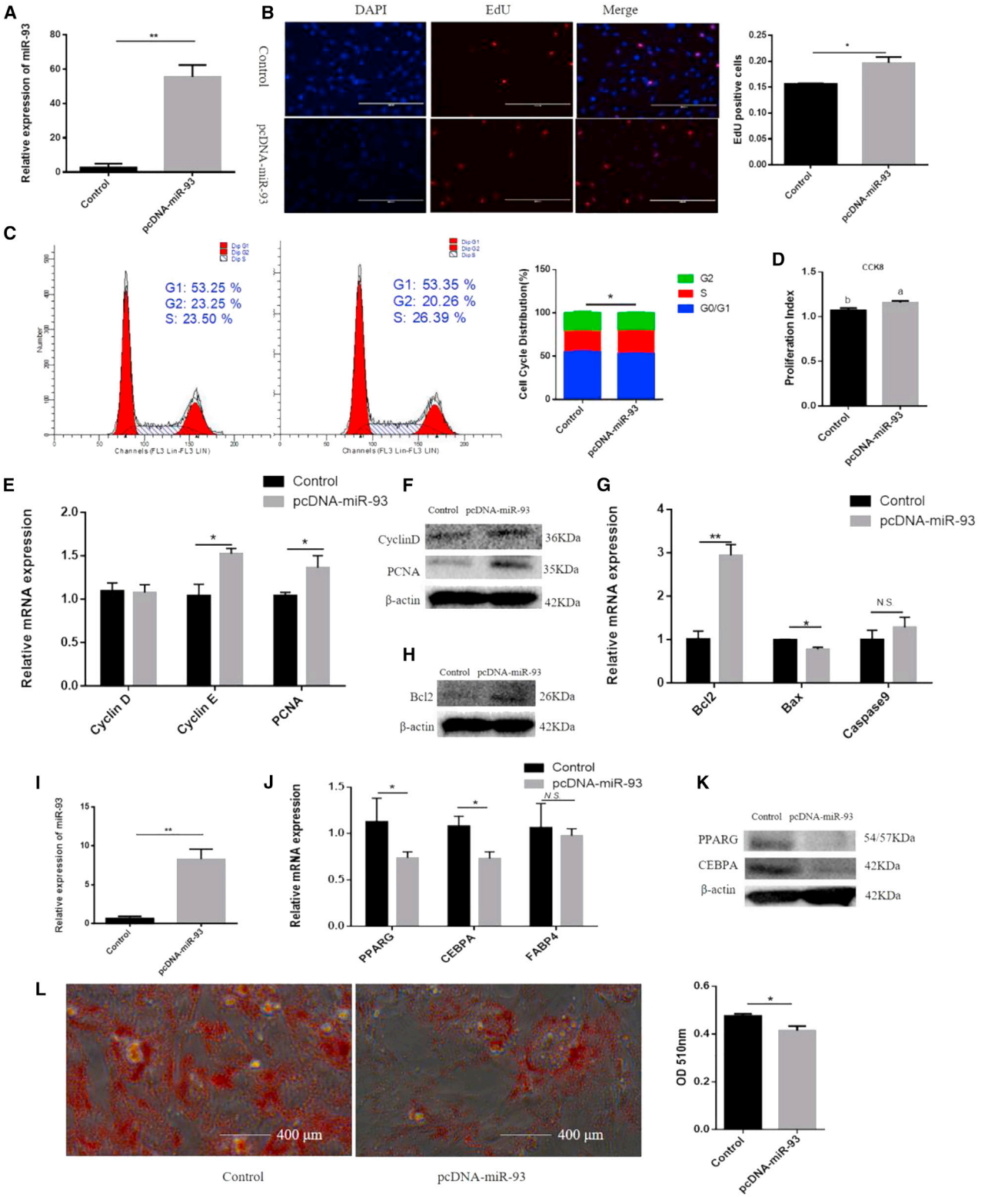

(legend on next page)

lncSLC30A9 and miR-93 (Figure 3H). Furthermore, the semiquantitative PCR results demonstrated that *lncSLC30A9* was expressed in the nucleus and cytoplasm (Figure 3I). The above data revealed that *lncSLC30A9* is a potential target of miR-93.

Effects of *lncSLC30A9* on Adipocyte Proliferation, Apoptosis, and Differentiation

We examined the expression of *lncSLC30A9* and its maternal gene (*SLC30A9*) in different tissues of the fetus, calf, and adult cattle during different differentiation periods. *lncSLC30A9* was mainly expressed in the spleen of calves, while *SLC30A9* was mainly expressed in the liver of the fetus and lung of adults (Figures S4A and S4B). However, their expression patterns were consistent during adipogenic differentiation and showed an overall increasing trend (Figures S4C and S4D). In addition, we found that overexpression of *lncSLC30A9* did not affect the expression of the maternal gene (SLC30A9; Figure S4E). However, when *SLC30A9* was knocked down, the expression of *lncSLC30A9* decreased significantly (Figures S4F and S4G).

We overexpressed *lncSLC30A9a* and *lncSLC30A9b* and performed the EdU incorporation assay to detect cell proliferation. Detection of overexpression efficiency showed that *lncSLC30A9a* and *lncSLC30A9b* expression was markedly increased (Figure 4A). The data showed that *lncSLC30A9a* reduced mitotic activity in adipocytes (Figure 4B). The results of flow cytometry were consistent with these findings (Figure 4C). Furthermore, CCK-8 detection showed that *lncSLC30A9a* markedly inhibited cell viability (Figure 4D). In addition, the proliferation-related markers, including cyclinD, cyclinE, and *PCNA* mRNA and protein levels were significantly reduced after cells were transfected with pcDNA- *lncSLC30A9a* (Figures 4E and 4F).

Further detection assays showed that *lncSLC30A9b* significantly reduced the expression of Bcl-2 (Figures 4G and 4H). We also found that overexpressed *lncSLC30A9a* and *lncSLC30A9b* increased the expression levels of three adipocyte markers, PPARG, CEBPA, and FABP4, at day 6 (Figures 4I–4K). Consistent results were obtained with the Oil Red O staining assay (Figure 4L). These findings indicate that *lncSLC30A9* may have an important function in adipocyte development.

Overexpression of *circFLT1* and *lncCCPG1* Serves as a Competing Endogenous miRNA-93 Sponge to Attenuate Its Inhibition of *lncSLC30A9*

Based on the high-throughput sequencing data of circRNAs and lncRNAs in Qinchuan bovine adipocytes, we randomly selected 12 differentially expressed circRNAs that may interact with miR-93. The results of real-time qPCR analysis showed that the expression of three circRNAs was much higher in preadipocytes compared with mature adipocytes (Figure S5A; Figure 5A). Furthermore, only *circFLT1* (bta_circ_002673) cDNA was obtained via a divergent primer (Figure S5B; S.Z., unpublished data). The size and sequence of amplified PCR products were determined by Sanger sequencing (Figure 5B). We isolated total RNA of adipocytes treated with actinomycin D to analyze the stability and localization of *circFLT1*. The data illustrated that the half-life of *circFLT1* surpassed 12 h. However, the half-life of linear FLT1 was less than 4 h (Figure 5C). We also screened and identified a significantly upregulated lncRNA, *lncCCPG1*, according to its host gene cell cycle progression 1[5] (Figure 5D). Through bioinformatics analysis, we found that *lncCCPG1* has a large number of miR-93 binding sites. DNAAF4-CCPG1 lncRNA also exists in humans. The RACE assay showed that *lncCCPG1* is a 2,397 nt transcript, and the CPC predicted that *lncCCPG1* has extremely low coding potential (Figures S5C–S5E).

The semiquantitative PCR results demonstrated that *circFLT1* and *lncCCPG1* were mainly expressed in the cytoplasm (Figures 5E and 5F). Based on their subcellular location (in the cytoplasm), we speculated they employed the mechanism of miRNA adsorption to regulate gene expression. Therefore, we used the RNAhybrid tool to evaluate the capacity of *circFLT1* and *lncCCPG1* to bind to miRNAs, and the results revealed the presence miR-93 binding sites (Figures S5F and S5G). *CircFLT1* overexpression significantly reduced the expression of miR-93 in preadipocytes, and *lncCCPG1* knockdown significantly increased the expression of miR-93 in preadipocytes/adipocytes (Figures S5H–S5K). Moreover, the luciferase assay showed that miR-93 inhibited Rluc expression of psiCHECK2-circFLT1-WT and psiCHECK2-lncCCPG1-WT constructs (Figures 5G and 5H). The sensor assays further confirmed the above results (Figures 5I–5K). To determine whether the potential mechanisms of *circFLT1* and *lncCCPG1* during adipogenesis were related to miR-93-mediated regulation of *lncSLC30A9*, we used psiCHECK2-lncSLC30A9 as a sensor. As expected, the results were consistent with previous findings (Figures 5L and 5M). *circFLT1* overexpression significantly reduced the expression of *lncSLC30A9*, and *lncCCPG1* knockdown significantly increased the expression of *lncSLC30A9* (Figures S5L and S5M). Thus, *circFLT1* and *lncCCPG1* acted as molecular sponges to relieve the inhibitory effects of miR-93 on the expression of *lncSLC30A9*.

Effects of *circFLT1* and *lncCCPG1* on Cell Proliferation, Apoptosis, and Differentiation

To explore the functions of *circFLT1* and *lncCCPG1* in adipogenesis, we overexpressed *circFLT1* and knocked down *lncCCPG1* to detect cell proliferation (Figures 6A and 6B). The EdU incorporation assay showed that *circFLT1* reduced the mitotic activity of adipocytes, whereas the

Figure 2. Effect of miR-93 Overexpression on Adipocytes Proliferation, Apoptosis, and Differentiation

(A) Overexpression efficiency of miR-93. (B) Cell proliferation was measured with 5-ethynyl-20-deoxyuridine (EdU). (C) Cell phases analyzed by flow cytometry. (D) Cell proliferation index was measured by the cell counting kit-8 (CCK-8) assay. (E and F) Expression of the proliferation marker genes were measured with RT-qPCR (E) and western blotting (F). (G and H) Expression of the apoptosis marker genes were measured with RT-qPCR (G) and western blotting (H). (I) Overexpression efficiency of miR-93. (J and K) The mRNA and protein expression of cell differentiation markers were measured with RT-qPCR (J) and western blotting (K). (L) Oil Red O staining was used to detect the production of lipid droplet. Values are presented as mean ± SEM for three biological replicates. Different letters (a, b) represent significant differences as follows: $p < 0.05$; *$p < 0.05$; **$p < 0.01$. N.S., not significant.

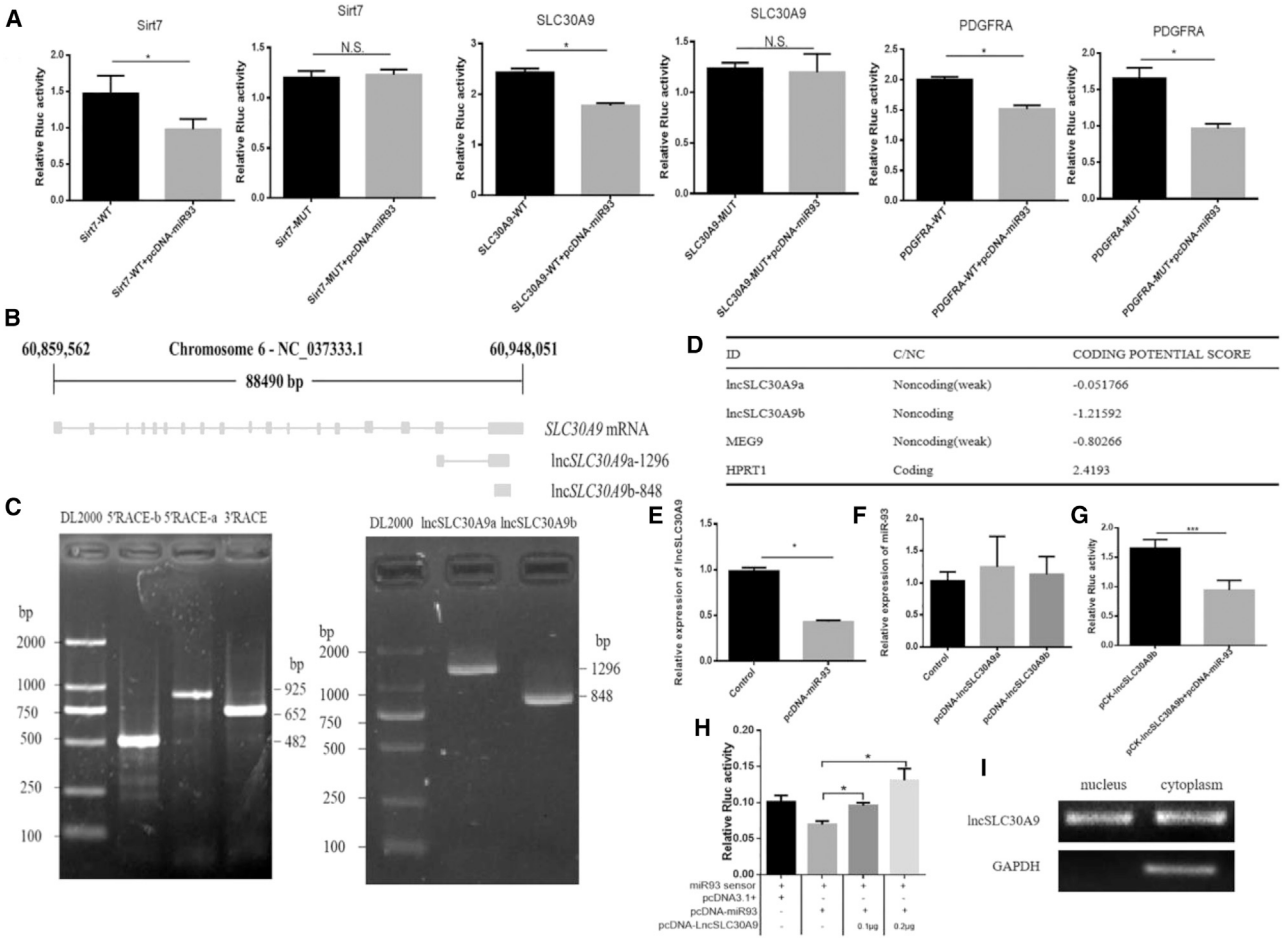

Figure 3. *lncSLC30A9* is a Target of miR-93

(A) HEK293T cells were cotransfected with the wild-type or mutant *Sirt7/SLC30A9/PDGFRA* dual-luciferase vector and PCDNA-miR-93, and the relative luciferase activity was analyzed 24 h after transfection. (B) Genomic structure of *lncSLC30A9*. (C) The 5′RACE and 3′RACE analyses demonstrated the full length of *lncSLC30A9*. (D) The RNA sequences of *lncSLC30A9a/ lncSLC30A9b* were processed by the Coding Potential Calculator (CPC) program. (E and F) The mRNA expression of *lncSLC30A9* (E) and miR-93 (F) were measured via RT-qPCR. (G) The PCDNA-miR-93 was cotransfected with pCK-lncSLC30A9 into HEK293T cells. Then, the relative luciferase activity was analyzed 24 h after the transfection. (H) The miR-93 sensor was cotransfected with the PCDNA-miR-93 and/or pcDNA-SLC30A9 into HEK293T cells. Double luciferase activity analysis. (I) Distribution of lncSLC30A9 after separation of nucleus and cytoplasm. Values are presented as mean ± SEM for three biological replicates. *$p < 0.05$, **$p < 0.001$. N.S., not significant.

overexpression of miR-93 slightly reversed these effects (Figure 6C). In contrast, *si-lncCCPG1* promoted cell proliferation (Figure 6D). The results of flow cytometry, CCK-8, real-time qPCR, and western blotting were all consistent (Figures 6E–6L). Considering that miR-93 can inhibit apoptosis, we further investigated whether *circFLT1* and *lncCCPG1* can affect the apoptosis of adipocytes by regulating miR-93. Notably, *circFLT1* also reduced the expression of Bcl-2, which was increased after co-transfection with miR-93 (Figures 6M and 6N). However, *lncCCPG1* had no significant effects on apoptosis (Figures 6O and 6P). Furthermore, *circFLT1* overexpression increased the expression of PPARG, CEBPA, and FABP4, and miR-93 overexpression slightly reversed these effects (Figures 7A–7C). However, *si-lncCCPG1* showed the opposite effect (Figures 7D–7F). Consistent results were obtained via the Oil Red O staining assay (Figure 7G and 7H). Furthermore, *lncCCPG1* overexpression inhibited cell proliferation and promoted differentiation (Figure S6). The above data show that *circFLT1* and *lncCCPG1* can suppress adipocyte proliferation and promote differentiation by adsorbing miR-93.

To explore the regulatory mechanism of *lncCCPG1* at the transcriptional level, we predicted its activity with the aid of the UCSC Genome Browser. We found that H3K4me1 and H3K27ac were used in the upstream region of *lncCCPG1* (Figure S7A). Therefore, five reporter genes containing different *lncCCPG1* promoter fragments were constructed for luciferase detection; however, no promoter active region was detected (Figure S7B).

We then connected the upstream region (−1416∼−721) to the enhancer region to detect its activity and found this region to show significant enhancer activity (Figure S7C). The combined predicted results from

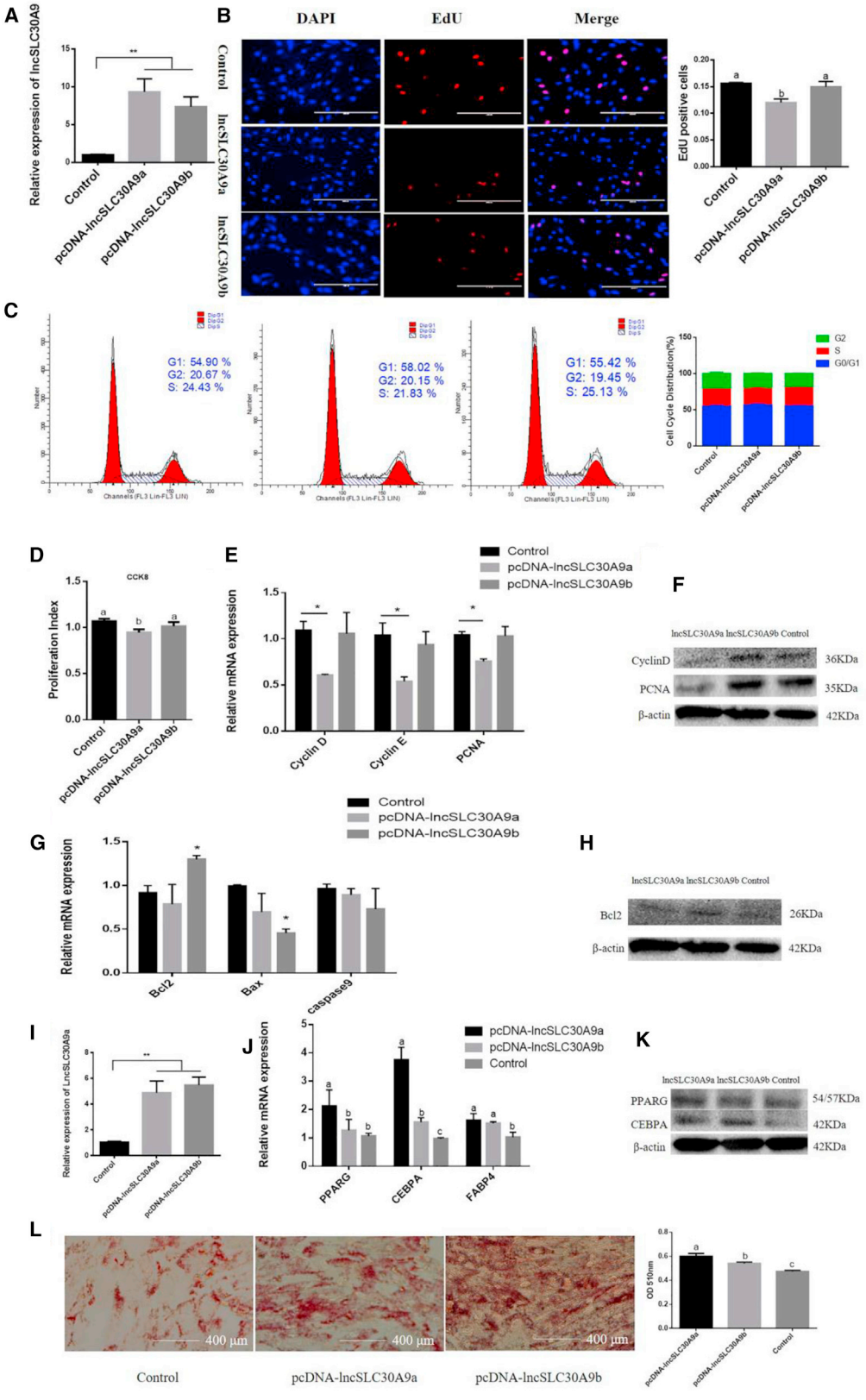

(legend on next page)

the UCSC and JASPAR databases showed that the FOXA1 and FOS protein binding sites might exist in this region. Following the overexpression of FOS and knockdown of FOXA1, we observed that *FOS* significantly enhanced the fluorescence activity of this region, while FOXA1 showed no significant change in the fluorescence activity in this same region (Figure S7D). Further detection of changes in the expression of *lncCCPG1* revealed that FOS significantly promoted the expression of *lncCCPG1*, while si-FOXA1 did not significantly alter the expression of *lncCCPG1* (Figure S7E). The transcription factor, FOS, can bind to the enhancer region of *lncCCPG1* to promote the expression of *lncCCPG1*.

CircFLT1/lncCCPG1 Sponges the miR-93-lncSLC30A9-AKT/FOS Axis to Regulate Adipocyte Proliferation and Differentiation

To further explore the mechanisms of *circFLT1/lncCCPG1*, the PI3K-AKT signaling pathway was screened using the Kyoto Encyclopedia of Genes and Genomes (Figure 8A). Moreover, *lncSLC30A9a* and *lncSLC30A9b* overexpression significantly inhibited AKT phosphorylation. However, no significant change was detected at day 6 of differentiation (Figure 8B). Based on these results, we hypothesized that *lncSLC30A9* inhibits proliferation by inhibiting the activation of the AKT signaling pathway.

Studies have shown that some lncRNAs play a functional role by interacting with specific proteins. The nuclear localization of *lncSLC30A9* suggests that lncRNA might play a regulatory role by interacting with proteins. Therefore, the potential *lncSLC30A9* binding protein was predicted using the RNA-Protein Interaction Prediction (RPISeq) tool. The results showed that *lncSLC30A9* can bind the FOS protein (Figure 8C). The FOS overexpression vector was also transfected into adipocytes, and the *lncSLC30A9* expression level was significantly upregulated (Figure 8D). However, the overexpressed *lncSLC30A9a* and *lncSLC30A9b* vectors were transfected into fat cells, and the *FOS* gene showed no significant change in mRNA levels but showed significantly increased protein levels (Figures 8E and 8F).

The FOS protein was also expressed at different periods of fat differentiation in Qinchuan cattle, showing a tendency to increase and then decline; its highest expression was observed on day 6 of differentiation (Figure 8G). Previous studies have shown that FOS can bind to the *PPARG* promoter. In differentiated adipocytes, the binding activity of FOS to the PPARG promoter was significantly increased, revealing the potential role of FOS in the transcriptional regulation of *PPARG* in adipocyte differentiation.[9]

We further examined the effects of FOS on the proliferation and differentiation of adipocytes. The real-time qPCR and western blotting analyses showed that FOS had no significant effects on cell proliferation but was able to significantly promote cell differentiation. More lipid droplets were detected in the pcDNA-FOS-transfected adipocytes via Oil Red O staining on day 6 of differentiation (Figure S8). Overall, these results indicated that *circFLT1* and *lncCCPG1* regulate the proliferation and differentiation of bovine adipocyte by the *circFLT1/lncCCPG1-miR-93-lncSLC30A9-AKT/FOS* axis (Figure 9).

DISCUSSION

Previous studies have underlined the significance of ncRNAs in adipogenesis, especially in regulating the proliferation and differentiation of adipocytes.[10–13] The expression of ncRNAs is specific to cells and tissues and may differ between various stages of differentiation. This observation suggests that ncRNAs may be fine-tuning factors of cell fate. Research on ncRNAs has been mainly focused on tumorigenesis and the pluripotency of stem cells. However, much remains to be learned about the functions of ncRNAs in adipocyte formation and particularly the regulation of adipocyte differentiation.

In this study, we found three adipocyte differentiation-related ncRNAs (*circFLT1*, *lncCCPG1*, and *lncSLC30A9*) that facilitate adipogenesis. By functioning as competing endogenous RNAs (ceRNAs), *circFLT1* and *lncCCPG1* overexpression released the inhibitory effects of miR-93 on lncSLC30A9 through the adsorption of miR-93 and thereby increased the expression of *lncSLC30A9*. This increase in *lncSLC30A9* expression further activates the lncSLC30A9-AKT/FOS axis to regulate adipocyte proliferation and differentiation.

Previous work suggests that miRNAs play an important role in regulating biological processes.[14,15] However, the functions of many miRNAs in bovine fat production are not entirely understood. In this study, a miRNA was identified from high-throughput miRNA sequencing data from various differentiation intervals in Qinchuan cattle. Compared with other miRNAs, miR-93 expression was significantly upregulated at day 6 of differentiation. Therefore, we speculated that miR-93 may regulate adipogenesis.

Previous studies have shown that miR-93 can regulate many cancers, but, to our knowledge, there are no reports on its effects on bovine fat development.[16,17] Cioffi et al. reported that miR-93 controls obesity by inhibiting Sirt7 and Tbx3.[7] The current study showed that miR-93 regulates both the proliferation and differentiation of bovine adipocytes. Consider that miR-93 is highly conserved among cows, mice, and humans. Therefore, we also checked its function in 3T3-L1 cells (a well-characterized model of mouse adipogenesis). We noted that the findings were entirely consistent with those of bovine adipocyte studies. These results may

Figure 4. Effect of *lncSLC30A9* Overexpression on Adipocytes Proliferation, Apoptosis, and Differentiation

(A) Overexpression efficiency of *lncSLC30A9a* and *lncSLC30A9b*. (B) Cell proliferation was measured using 5-ethynyl-20-deoxyuridine (EdU). (C) Cell phase analyzed by flow cytometry. (D) Cell proliferation index was measured using the cell counting kit-8 (CCK-8) assay. (E and F) Expression of the proliferation marker genes were measured with RT-qPCR (E) and western blotting (F). (G and H) Expression of the apoptosis marker genes were measured with RT-qPCR (G) and western blotting (H). (I) Overexpression efficiency of *lncSLC30A9a* and *lncSLC30A9b*. (J and K) The mRNA and protein expression of cell differentiation markers were measured with RT-qPCR (J) and western blotting (K). (L) Oil Red O staining was used to detect the production of lipid droplet. Values are presented as mean ± SEM for three biological replicates. Different letters (a, b, and c) represent significant differences as follows: $p < 0.05$; $^{*}p < 0.05$; $^{**}p < 0.01$, respectively.

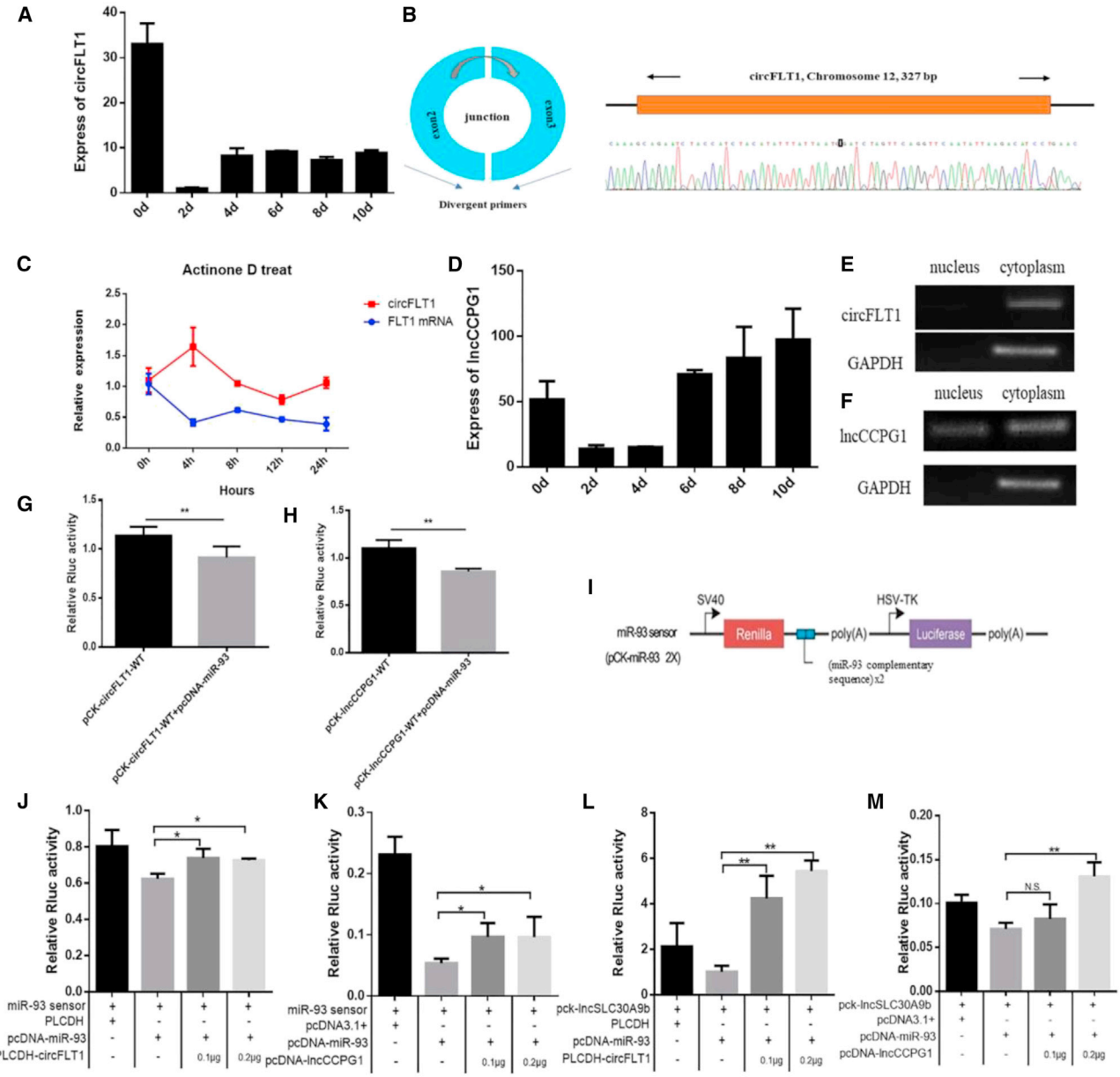

Figure 5. Analysis of the interaction between *circFLT1*/ *lncCCPG1* and miR-93

(A and D) Expression of *circFLT1* (A) or *lncCCPG1* (D) in various differentiation intervals in the adipocytes of Qinchuan cattle. (B) Structural analysis of *circFLT1*. (C) Levels of *circFLT1* and linear *FLT1* expression in adipocytes treated with actinomycin D (1 μg/mL) were detected by RT-qPCR at the indicated time points. (E and F) Distribution of *circFLT1* (E) or *lncCCPG1* (F) after separation of nucleus and cytoplasm. (G and H) pcDNA3.1-miR-93 was co-transfected with psi-Check2-*circFLT1* (G) or psi-Check2-*lncCCPG1* (H) into 293T cells. (I–K) Sensor construct of miR-93 (I); co-transfection with psi-Check2-*circFLT1* (J)/ psi-Check2-*lncCCPG1* (K) and the miR-93 sensor. (L, M) Co-transfection with psi-Check2-*circFLT1* (L)/ psi-Check2-*lncCCPG1* (M) and psi-Check2-*lncSLC30A9*. Values are presented as mean ± SEM for three biological replicates; *$p < 0.05$; **$p < 0.01$. N.S., not significant.

provide a new theoretical basis for the functions of miR-93 in adipogenesis. To our knowledge, this is the first study to identify miR-93 as a potential miRNA that can negatively regulate bovine fat production.

TargetScan analysis showed that miR-93 can directly target *lncSLC30A9*. The accuracy of this result was further verified by the dual-luciferase reporting system, and the molecular mechanism of miR-93 regulation of fat generation was preliminarily explored. To explore the function of *lncSLC30A9* in bovine adipocytes, we overexpressed *lncSLC30A9 in vitro* and transfected it into bovine adipocytes. The overexpressed *lncSLC30A9* may promote adipocyte differentiation and inhibit proliferation by increasing the expression of PPARG,

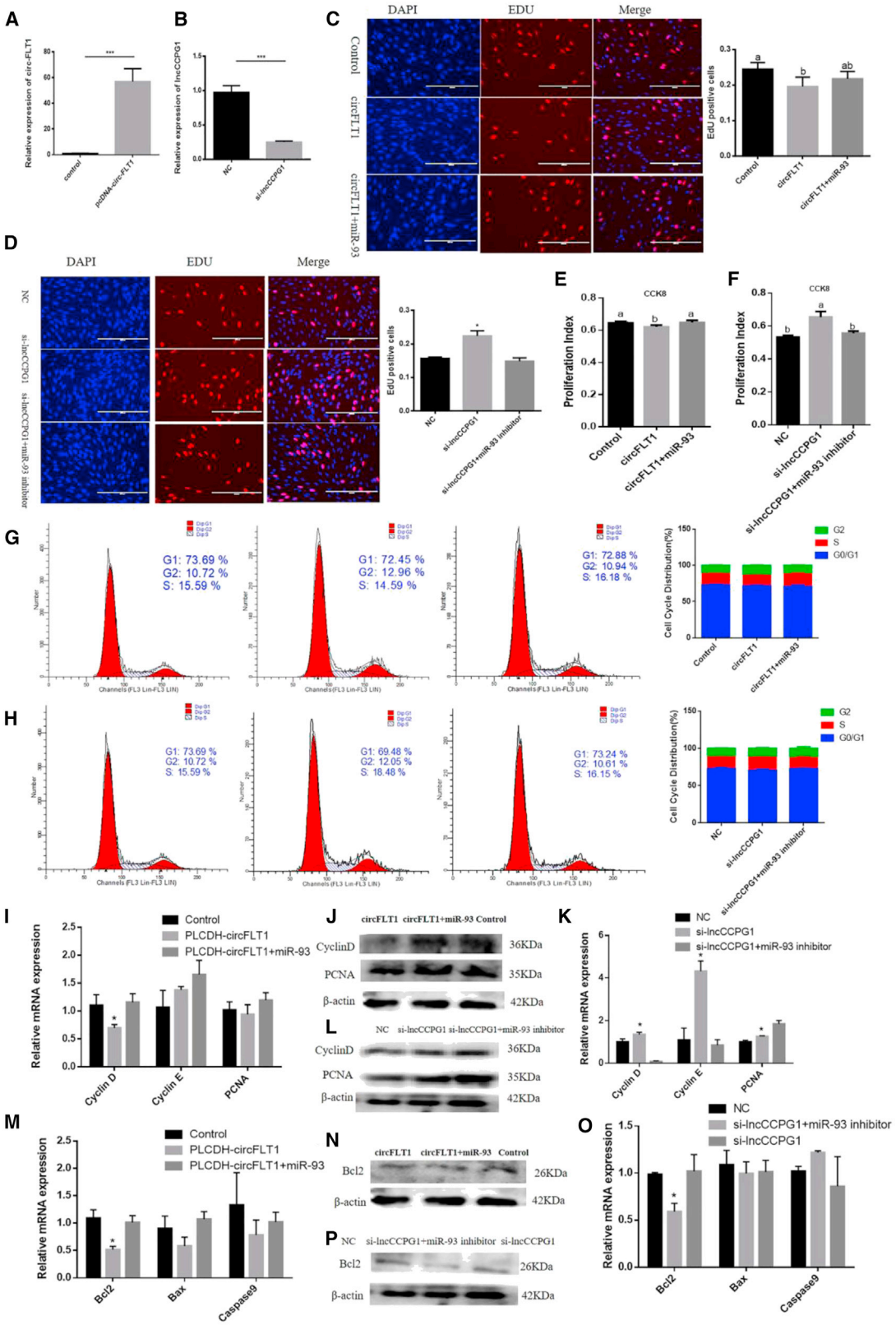

(legend on next page)

CEBPA, and FABP4, which is consistent with the function of overexpressed miR-93. Although the regulatory effects of miR-93 on fat production in Qinchuan cattle have been preliminarily revealed, additional studies on its mechanism of action are needed.

Previous studies have shown that circRNAs and lncRNAs can participate in post-transcriptional regulation through the competitive binding of miRNAs.[18] Some studies have shown that circRNAs can bind to many miRNAs to participate in normal growth and development.[19] However, only a few bovine circRNAs, such as circSNX29, have been shown to play a key role in growth.[10] Studies on the role of circRNAs in fat development have been rarely conducted. Although lncRNAs reportedly regulate adipocyte differentiation, the details of many regulatory mechanisms remain unclear.

In this study, sequencing data on circRNAs and lncRNAs revealed that *circFLT1* was downregulated, and *lncCCPG1* upregulated, during adipogenic differentiation. Nucleosomal separation revealed that both *circFLT1* and *lncCCPG1* were located mainly in the cytoplasm. Therefore, we analyzed the potential miRNA of *circFLT1* and *lncCCPG1* using bioinformatics tools and confirmed that they both had direct adsorption targets in miR-93 bovine fat cells using the dual-luciferase reporting system.

In addition, we found that *circFLT1* and *lncCCPG1* play a regulatory role in the proliferation of fat cells by regulating the removal of miR-93 from fat cells. More importantly, we found that the overexpression of *circFLT1* and *lncCCPG1* significantly promotes adipocyte differentiation, while the overexpression of miR-93 slightly reverses these effects. In addition, interference with *lncCCPG1* significantly promotes the expression of miR-93 and further inhibits adipocyte differentiation. Therefore, the overexpression of *circFLT1* and *lncCCPG1* leads to reduced activity of miR-93, disabling the inhibitory effect of miR-93 on the downstream target gene *lncSLC30A9*.

Therefore, *circFLT1* and *lncCCPG1* may indirectly increase the mRNA and protein levels of PPARG, CEBPA, and FABP4 and thereby promote adipocyte differentiation. In sum, these results further confirm that *circFLT1* and *lncCCPG1* may play a role in regulating the proliferation and differentiation of adipocytes through the competitive binding of miR-93. However, the present study only preliminarily discussed whether *circFLT1* and *lncCCPG1* can competitively adsorb miR-93 to regulate the proliferation and differentiation of adipocytes. Further in-depth studies on systematic mechanisms are necessary.

Previous studies have reported that some signaling pathways also participate in the regulation of cell proliferation and differentiation and that circRNAs and lncRNAs in the nucleus may play a role by interacting with proteins.[20–22] The present study showed that *circFLT1/lncCCPG1* could significantly increase the expression of its downstream target gene, *lncSLC30A9*, through the competitive adsorption of miR-93, leading to the question as to whether *lncSLC30A9* can also activate certain signaling pathways or recruit certain proteins to function within fat cells.

Generally, adipogenic differentiation is rigidly regulated by the activity of transcription factors, which can either activate or inhibit each other. The C/EBP family members (C/EBPA, C/EBPB, and C/EBPD) and PPARG are major transcription factors that are involved in adipogenesis.[23] The present study showed that overexpression of *circFLT1* or *lncCCPG1* in bovine fat cells could disarm the inhibitory effects of miR-93 on *lncSLC30A9*.

Furthermore, *lncSLC30A9* can be regulated by the recruitment of the FOS protein. The FOS protein can reportedly bind to the *PPARG* promoter. In differentiated adipocytes, the binding activity of c-*fos* to the *PPARG* promoter is significantly increased, indicating the potential role of c-*fos* in the transcriptional regulation of *PPARG* in adipocyte differentiation.[9] The potential lncSLC30A9 binding proteins were predicted using the RPISeq algorithm, revealing that *lncSLC30A9* could bind the FOS protein.

In addition, the FOS overexpression vector was transfected into adipocytes, and the *lncSLC30A9* expression level was significantly upregulated, whereas the overexpression of *lncSLC30A9a* and *lncSLC30A9b* was significantly upregulated. The *FOS* gene showed no significant change at the mRNA level but was significantly increased at the protein level. More importantly, overexpression of *circFLT1* or *lncCCPG1* may inhibit proliferation by inhibiting the AKT signaling pathway and, in combination with miR-93, may promote differentiation by recruiting the FOS protein to the *PPARG* promoter.

In sum, we identified the adipogenesis-associated *circFLT1* and *lncCCPG1* and found that they can promote adipocyte differentiation and inhibit proliferation *in vitro*. Specifically, overexpression of *circFLT1* or *lncCCPG1* can act as a ceRNA, adsorb miR-93 to remove its inhibitory effects on *lncSLC30A9*, and increase the expression of *lncSLC30A9*. Furthermore, *lncSLC30A9* inhibits proliferation by inhibiting the activation of the AKT signaling pathway and promotes differentiation by recruiting the FOS protein to the *PPARG* promoter. However, additional studies are needed to determine whether *circFLT1* and *lncCCPG1* are associated with other regulatory processes and whether their regulatory approaches to adipocyte differentiation are conserved in humans and mice.

Figure 6. Effects of *circFLT1* and *lncCCPG1* on Adipocytes Proliferation and Apoptosis

(A and B) Overexpression/knockdown efficiency of *circFLT1* (A) and *lncCCPG1* (B) on cell proliferation. (C and D) Cell proliferation was measured with the 5-ethynyl-20-deoxyuridine (EdU) assay of *circFLT1* (C) and *lncCCPG1* (D). (E and F) The cell proliferation index was measured by the cell counting kit-8 (CCK-8) assay of *circFLT1* (E) and *lncCCPG1* (F). (G and H) Cell phases were analyzed using flow cytometry of *circFLT1* (G) and *lncCCPG1* (H). (I–L) Expression of proliferation marker genes was measured with RT-qPCR of *circFLT1* (I) and *lncCCPG1* (K) and western blotting of *circFLT1* (J) and *lncCCPG1* (L). (M–P) Expression of apoptosis marker genes was measured with RT-qPCR of *circFLT1* (M) and *lncCCPG1* (O) and western blotting of *circFLT1* (N) and *lncCCPG1* (P). Values are presented as mean ± SEM for three biological replicates. Different letters (a, b) indicate significant differences: $p < 0.05$; *$p < 0.05$; ***$p < 0.001$.

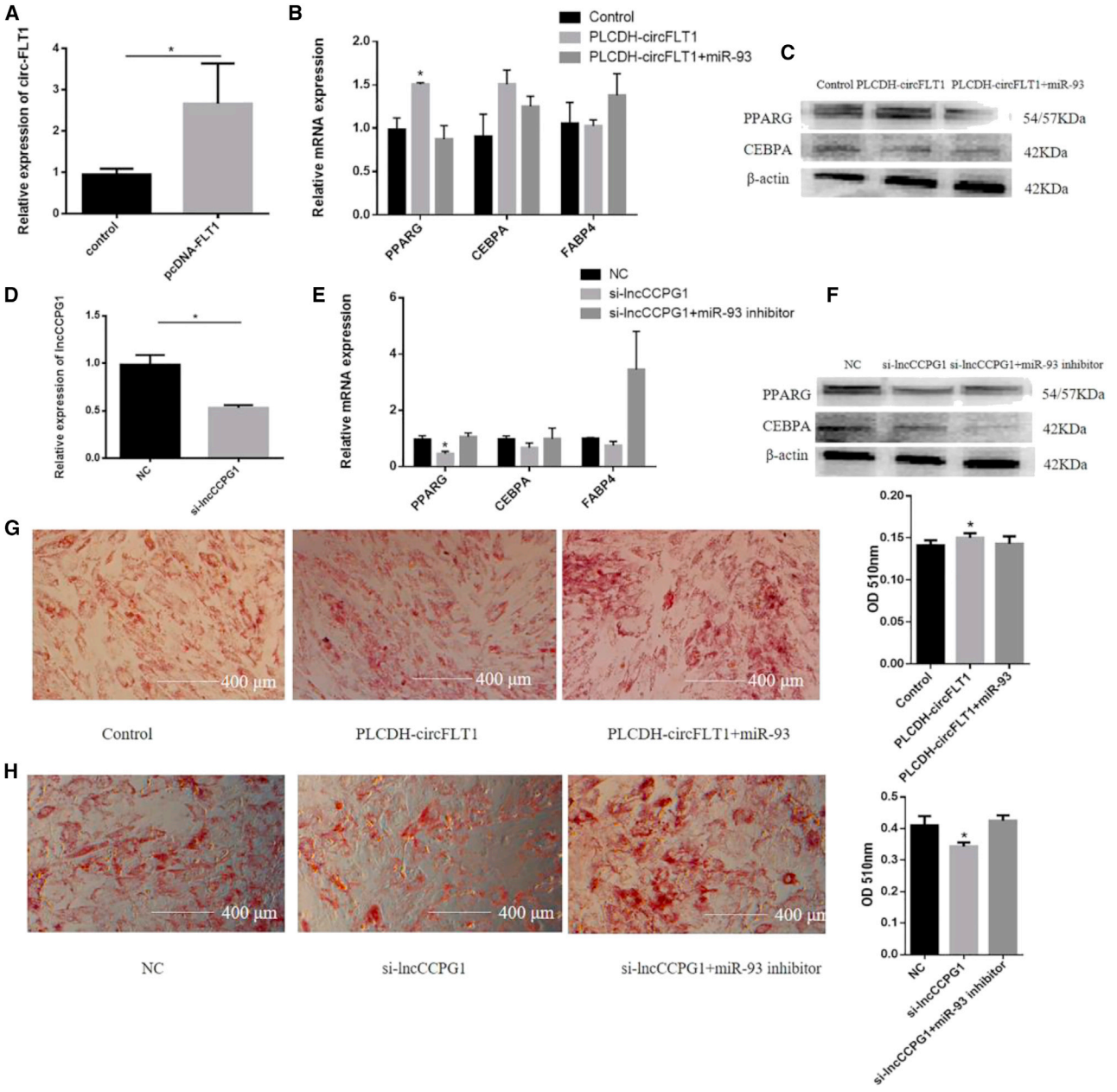

Figure 7. Effects of *circFLT1* and *lncCCPG1* on Adipocytes Differentiation

(A and D) Overexpression/knockdown efficiency of *circFLT1* (A) and *lncCCPG1* (D) on cell differentiation. (B and C) The mRNA and protein expressions of cell differentiation markers were measured with RT-qPCR (B) and western blotting of *circFLT1* (C). (E and F) The mRNA and protein expressions of cell differentiation markers were measured with RT-qPCR (E) and western blotting (F) of *lncCCPG1*. (G and H) Oil Red O staining was used to detect the production of lipid droplets of *circFLT1* (G) and *lncCCPG1* (H). Values are presented as mean ± SEM for three biological replicates. *$p < 0.05$.

MATERIALS AND METHODS

Sample Preparation

All animal experiments in this study were approved by the Faculty Animal Policy and Welfare Committee of Northwest A&F University (No. NWAFAC1008). The care and use of experimental animals were in full compliance with local animal welfare laws, guidelines, and policies.

Tissue samples were collected from the slaughterhouse in Xi'an. Subcutaneous adipose tissue was resected and immediately placed in

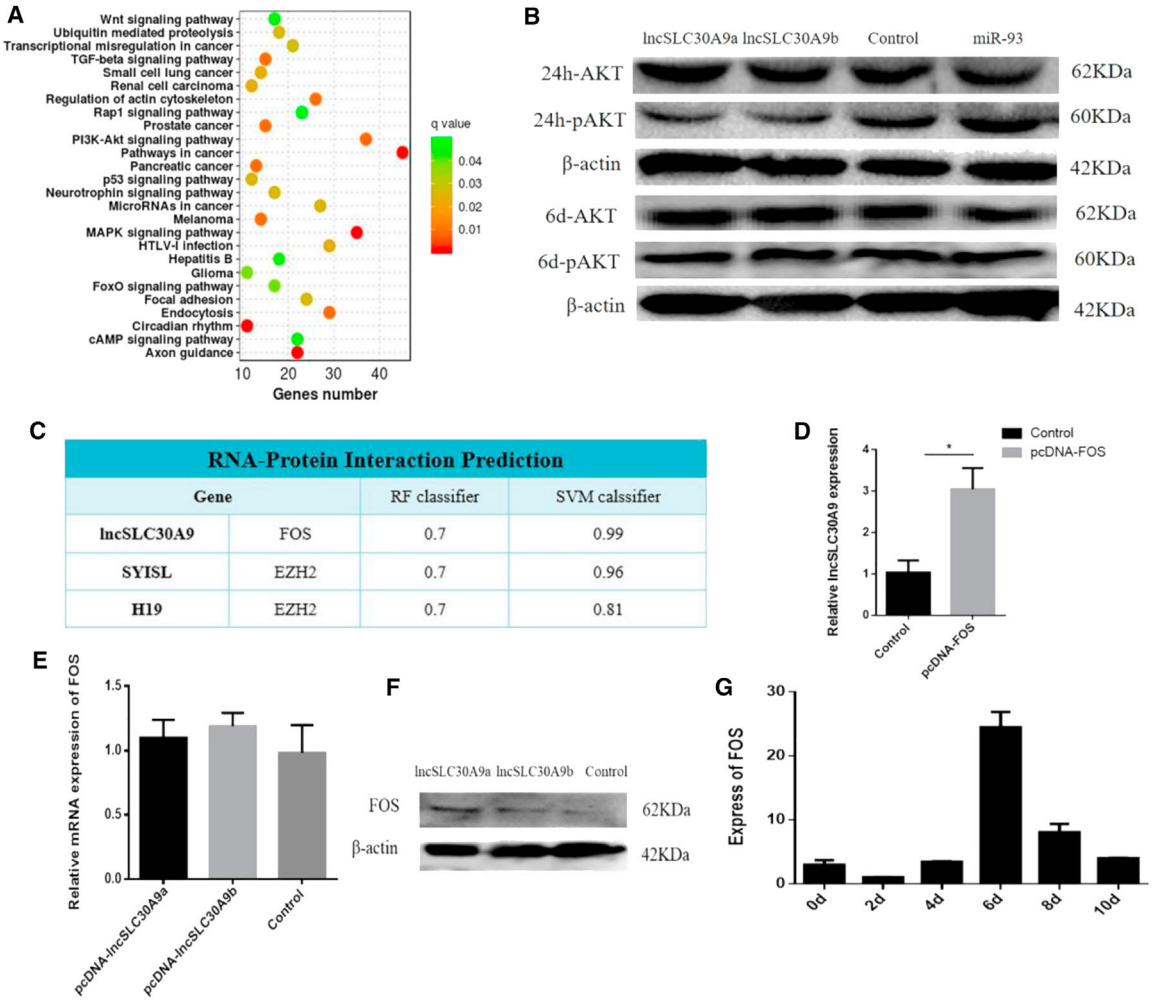

Figure 8. *circFLT1/lncCCPG1* Regulates the miR-93-lncSLC30A9-AKT/FOS Axis to Affect Adipocyte Proliferation and Differentiation

(A) Kyoto Encyclopedia of Genes and Genomes enrichment analysis results. (B) Detection of AKT and pAKT by western blotting. (C) The RNA-Protein Interaction Prediction (RPISeq) result. (D) The mRNA expression of *lncSLC30A9* was detected by real-time qPCR. (E) The mRNA expression of *FOS* was detected by real-time qPCR. (F) The protein expression of FOS was detected by western blotting. (G) The expression of *FOS* at various differentiation intervals in the adipocytes of Qinchuan cattle. Values are presented as mean ± SEM for three biological replicates; *$p < 0.05$.

Dulbecco's modified Eagle's medium at 37°C and taken back to the laboratory for primary adipose cell separation.

Cell Culture

Adipocytes were isolated from bovine subcutaneous adipose tissue. The specific separation was performed following the methods of a previous study.[24] The cells were seeded in a medium containing 20% fetal bovine serum and 1% antibiotics in 5% CO_2 at 37°C. HEK293T (human embryonic kidney 293) cells and 3T3-L1 cells (a preadipocyte cell line derived from the Swiss 3T3 mouse fibroblast cell line) were cultured in 10% fetal bovine serum and 1% penicillin-streptomycin, which were provided by our laboratory.

RNA Isolation and Real-Time qPCR

Total RNA from tissues and cell lysates was isolated using the TRIzol reagent and was stored at −80°C (Takara, Dalian, China).[25] Real-time qPCR was conducted using the SYBR green detection dye and CFX96 Real-Time PCR Detection System. The PCR protocol was similar to that described by Li et al.[26] Primer information is presented in Table S1. The $2^{-\Delta\Delta Ct}$ method was used to analyze the relative expression levels of real-time qPCR data.

RACE

RACE amplification was conducted to determine the complete fragments of *lncCCPG1* and *lncSLC30A9* using the SMARTer RACE cDNA Amplification Kit (Clontech, Palo Alto, CA, USA). Total

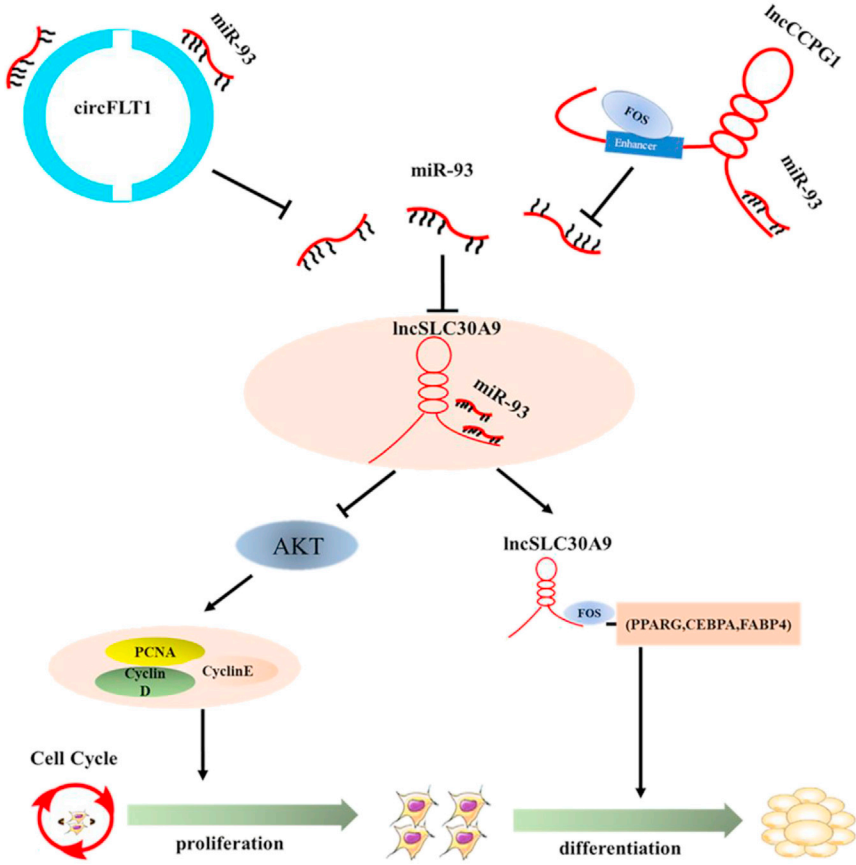

Figure 9. Proposed Working Model by which circFLT1 and lncCCPG1 Regulate Adipogenesis

RNA was obtained from bovine adipocytes per the manufacturer's instructions.

Plasmid Construction

The full lengths of *circFLT1*, *lncCCPG1*, and *lncSLC30A9*, including miR-93, were cloned into pLCDH-circRNA or pcDNA3.1(+) vectors, respectively. The *circFLT1* and *lncCCPG1* 3′ UTR fragments were amplified by PCR and included the miR-93-binding site. The fast enzymes, Not I and Xho I, were used to connect two fragments to the psiCHECK-2 (pCK) vector, which was then ligated by T4 DNA ligase. We consistently generated the plasmids of psiCHECK2 (pCK)-circFLT1-WT, psiCHECK2 (pCK)-lncCCPG1-WT, psiCHECK2 (pCK)-lncSLC30A9-WT, psiCHECK2 (pCK)-SLC30A9-WT/Mut, psiCHECK2 (pCK)-Sirt7-WT/Mut, and psiCHECK2(pCK)-PDGFRA-WT/Mut. The wild-type fragment was directly amplified by PCR amplification, including the miR-93-binding site. The seed sequence was randomly mutated to prevent the binding of miR-93, and the mutant sequence was designed with the reverse primer. Primer information is provided in Table S1.

Luciferase Activity Assay

The HEK293T cells were inoculated in 96-well plates. When cell fusion was approximately 50%, cells were co-transfected with miR-93 and pCK-circFLT1-Wild or pCK-lncCCPG1-Wild. The cells were then cultured in twice the volume of medium for 24 h. The miR-93 sensor was constructed by inserting two miR-93 complementary sequences into the pCK vector. Similarly, adipocytes were inoculated in 96-well plates and co-transfected with a wild-type construct of *lncSLC30A9/SLC30A9/Sirt7/PDGFRA* with or without miR-93. Luciferase activity was determined per the manufacturer's instructions for the luciferase reporter assay kit (Promega).

Cell Proliferation Assay

In the CCK-8 assay, the preadipocytes were seeded into a 96-well plate and further cultured until the cell density was approximately 50%. Plasmids (100 ng) were then transfected into the cells and cultured for 24 h with double complete medium. When the cell density reached approximately 75%, 10 μL of CCK-8 reagent was added to each well, and cells were cultured for 2–4 h. After gentle shaking, the optical density was immediately detected at a wavelength of 450 nm for further statistical analyses. In the EdU assay, preadipocytes were inoculated in a 48-well plate. When the cell density was 50%, plasmids (200 ng) were transfected into the cells, which were then cultured for 24 h. The EdU medium was added to each well, and cells were fixed after 3 h of culture. Cells were detected with the aid of a microscope.[27] For the cell cycle assay, preadipocytes were cultured in a 60-cm^2 culture dish, to which 4 mL of medium was added. The cells were treated and transfected with plasmids (3 μg). After 24 h, adipocytes were fixed with 70% ethanol (ethanol:PBS = 7:3) overnight at −20°C. The cell suspension was evaluated with a cell cycle testing kit.

Adipogenic Differentiation and Oil Red O Staining

When cell confluence reached 100%, the medium was replaced with the induced differentiation medium. After 2 days, cells were incubated in the same differentiation medium, which was changed every 2 days.[24] After adipocyte differentiation was achieved, the medium was discarded, and cells were washed with PBS. Cells were fixed with 4% paraformaldehyde and left at room temperature for 30 min. The 4% paraformaldehyde solution was then discarded, and cells were washed three times and stained for 1 h in Oil Red O solution. The Oil Red O dye was then discarded, and the cells were immediately washed four times with PBS. Images were captured under a light microscope.[6]

Western Blotting Analysis

After the medium in the cell culture dish was discarded, the cells (about 10^6) were washed with PBS, digested with trypsin, and collected into a 1.5-mL centrifuge tube. After centrifugation, the supernatant was removed. The radioimmunoprecipitation assay cell lysate containing the phenylmethanesulfonylfluoride protease inhibitor was added at a ratio of 4:1 (Solarbio, Beijing, China). The protein was heated with sodium dodecyl sulfate (SDS)-loading buffer to 98°C for 10 min. The samples were added to SDS-polyacrylamide gel for electrophoretic separation and then transferred to 0.2-μm polyvinylidene difluoride (PVDF) membranes. After electrophoresis, the PVDF membranes were removed, washed with Tris-buffered saline + Tween 20 (TBST) solution for 10 min, and sealed with sealant for 2 h. The membranes were again washed three times with TBST solution, each time for 10 min. The membranes were incubated overnight with primary antibodies at 4°C and then washed three times with TBST. The PVDF membrane was then incubated with the secondary antibody at room temperature for 2 h.[27] Details of the antibodies are presented in Table S2.

Statistical Analysis

GraphPad Prism 8.0 (GraphPad, USA) and SPSS 24.0 (IBM Corp., NY, USA) were used for data analyses. All data were analyzed using one-way ANOVA or t tests. When $p < 0.05$, the difference was considered statistically significant. Data were presented as mean ± SEM.

SUPPLEMENTAL INFORMATION

Supplemental Information can be found online at https://doi.org/10.1016/j.omtn.2020.09.011.

AUTHOR CONTRIBUTIONS

X.L. and Z.K designed research. Z.K., S.Z., E.J., X.W., and Z.W. performed experiments and analyzed data. Z.K. wrote the paper. E.J. and X.W. contributed new analytic tools. X.L. and H.C. helped modify the language of this manuscript.

CONFLICTS OF INTEREST

The authors declare no competing interests.

ACKNOWLEDGMENTS

This work was supported by the National Natural Science Foundation of China (No. 31872331; No. 31672400). We greatly appreciated the Life Science Research Core Services (LSRCS) of Northwest A&F University (Northern Campus) for providing us with the platform.

REFERENCES

1. Ali, A.T., Hochfeld, W.E., Myburgh, R., and Pepper, M.S. (2013). Adipocyte and adipogenesis. Eur. J. Cell Biol. *92*, 229–236.
2. Berry, D.C., Stenesen, D., Zeve, D., and Graff, J.M. (2013). The developmental origins of adipose tissue. Development *140*, 3939–3949.
3. Cristancho, A.G., and Lazar, M.A. (2011). Forming functional fat: a growing understanding of adipocyte differentiation. Nat. Rev. Mol. Cell Biol. *12*, 722–734.
4. White, U.A., and Stephens, J.M. (2010). Transcriptional factors that promote formation of white adipose tissue. Mol. Cell. Endocrinol. *318*, 10–14.
5. Li, M., Sun, X., Cai, H., Sun, Y., Plath, M., Li, C., Lan, X., Lei, C., Lin, F., Bai, Y., and Chen, H. (2016). Long non-coding RNA ADNCR suppresses adipogenic differentiation by targeting miR-204. Biochim. Biophys. Acta *1859*, 871–882.
6. Jin, Y., Wang, J., Zhang, M., Zhang, S., Lei, C., Chen, H., Guo, W., and Lan, X. (2019). Role of bta-miR-204 in the regulation of adipocyte proliferation, differentiation, and apoptosis. J. Cell. Physiol. *234*, 11037–11046.
7. Cioffi, M., Vallespinos-Serrano, M., Trabulo, S.M., Fernandez-Marcos, P.J., Firment, A.N., Vazquez, B.N., Vieira, C.R., Mulero, F., Camara, J.A., Cronin, U.P., et al. (2015). MiR-93 controls adiposity via inhibition of Sirt7 and Tbx3. Cell Rep. *12*, 1594–1605.
8. Zhang, M., Li, F., Sun, J.W., Li, D.H., Li, W.T., Jiang, R.R., Li, Z.J., Liu, X.J., Han, R.L., Li, G.X., et al. (2019a). LncRNA IMFNCR Promotes Intramuscular Adipocyte Differentiation by Sponging miR-128-3p and miR-27b-3p. Front. Genet. *10*, 42.
9. Wang, X., Yang, P., Liu, J., Wu, H., Yu, W., Zhang, T., Fu, H., Liu, Y., and Hai, C. (2014). RARγ-C-Fos-PPARγ2 signaling rather than ROS generation is critical for all-trans retinoic acid-inhibited adipocyte differentiation. Biochimie *106*, 121–130.
10. Peng, S., Song, C., Li, H., Cao, X., Ma, Y., Wang, X., Huang, Y., Lan, X., Lei, C., Chaogetu, B., and Chen, H. (2019). Circular RNA SNX29 Sponges miR-744 to Regulate Proliferation and Differentiation of Myoblasts by Activating the Wnt5a/Ca^{2+} Signaling Pathway. Mol. Ther. Nucleic Acids *16*, 481–493.
11. Zhang, M., Li, B., Wang, J., Zhang, S., Li, H., Ma, L., Guo, W., Lei, C., Chen, H., and Lan, X. (2019b). lnc9141-a and -b Play a Different Role in Bovine Myoblast Proliferation, Apoptosis, and Differentiation. Mol. Ther. Nucleic Acids *18*, 554–566.
12. Jiang, R., Li, H., Yang, J., Shen, X., Song, C., Yang, Z., Wang, X., Huang, Y., Lan, X., Lei, C., and Chen, H. (2020). circRNA Profiling Reveals an Abundant circFUT10 that Promotes Adipocyte Proliferation and Inhibits Adipocyte Differentiation via Sponging let-7. Mol. Ther. Nucleic Acids *20*, 491–501.
13. Zhang, S., Kang, Z., Cai, H., Jiang, E., Pan, C., Dang, R., Lei, C., Chen, H., and Lan, X. (2020). Identification of novel alternative splicing of bovine lncRNA lncFAM200B and its effects on preadipocyte proliferation. J. Cell. Physiol. Published online June 15, 2020. https://doi.org/10.1002/jcp.29887.
14. Lu, J., Getz, G., Miska, E.A., Alvarez-Saavedra, E., Lamb, J., Peck, D., Sweet-Cordero, A., Ebert, B.L., Mak, R.H., Ferrando, A.A., et al. (2005). MicroRNA expression profiles classify human cancers. Nature *435*, 834–838.
15. Zhang, Z., Sun, H., Dai, H., Walsh, R.M., Imakura, M., Schelter, J., Burchard, J., Dai, X., Chang, A.N., Diaz, R.L., et al. (2009). MicroRNA miR-210 modulates cellular response to hypoxia through the MYC antagonist MNT. Cell Cycle *8*, 2756–2768.
16. Wu, H., Liu, L., and Zhu, J.M. (2019). MiR-93-5p inhibited proliferation and metastasis of glioma cells by targeting MMP2. Eur. Rev. Med. Pharmacol. Sci. *23*, 9517–9524.
17. Lan, L., Liang, Z., Zhao, Y., and Mo, Y. (2020). LncRNA MCM3AP-AS1 inhibits cell proliferation in cervical squamous cell carcinoma by down-regulating miRNA-93. Biosci. Rep. *40*, BSR20193794.
18. Yang, X., Wang, J., Zhou, Z., Jiang, R., Huang, J., Chen, L., Cao, Z., Chu, H., Han, B., Cheng, Y., and Chao, J. (2018). Silica-induced initiation of circular ZC3H4 RNA/ZC3H4 pathway promotes the pulmonary macrophage activation. FASEB J. *32*, 3264–3277.
19. Wei, X., Li, H., Yang, J., Hao, D., Dong, D., Huang, Y., Lan, X., Plath, M., Lei, C., Lin, F., et al. (2017). Circular RNA profiling reveals an abundant circLMO7 that regulates myoblasts differentiation and survival by sponging miR-378a-3p. Cell Death Dis. *8*, e3153.
20. Wang, X., Cao, X., Dong, D., Shen, X., Cheng, J., Jiang, R., Yang, Z., Peng, S., Huang, Y., Lan, X., et al. (2019a). Circular RNA TTN Acts As a miR-432 Sponge to Facilitate Proliferation and Differentiation of Myoblasts via the IGF2/PI3K/AKT Signaling Pathway. Mol. Ther. Nucleic Acids *18*, 966–980.
21. Wang, B., Zheng, J., Li, R., Tian, Y., Lin, J., Liang, Y., Sun, Q., Xu, A., Zheng, R., Liu, M., et al. (2019b). Long noncoding RNA LINC02582 acts downstream of miR-200c to promote radioresistance through CHK1 in breast cancer cells. Cell Death Dis. *10*, 764.
22. Jin, J.J., Lv, W., Xia, P., Xu, Z.Y., Zheng, A.D., Wang, X.J., Wang, S.S., Zeng, R., Luo, H.M., Li, G.L., and Zuo, B. (2018). Long noncoding RNA *SYISL* regulates myogenesis by interacting with polycomb repressive complex 2. Proc. Natl. Acad. Sci. USA *115*, E9802–E9811.
23. Lefterova, M.I., and Lazar, M.A. (2009). New developments in adipogenesis. Trends Endocrinol. Metab. *20*, 107–114.

24. Li, M.X., Sun, X.M., Zhou, Y., Wei, X.F., Sun, Y.J., Lan, X.Y., Lei, C., and Chen, H. (2015). Nicotinamide and resveratrol regulate bovine adipogenesis through a SIRT1-dependent mechanism. J. Funct. Foods *18*, 492–500.

25. Li, W., Liu, D., Tang, S., Li, D., Han, R., Tian, Y., Li, H., Li, G., Li, W., Liu, X., et al. (2019). A multiallelic indel in the promoter region of the Cyclin-dependent kinase inhibitor 3 gene is significantly associated with body weight and carcass traits in chickens. Poult. Sci. *98*, 556–565.

26. Li, W.Y., Jing, Z.Z., Cheng, Y.Y., Wang, X.N., Li, D.H., Han, R.L., Li, W., Li, G., Tian, Y., Liu, X., et al. (2020). Analysis of four complete linkage sequence variants within a novel lncRNA located in a growth QTL on chromosome 1 related to growth traits in chickens. J. Anim. Sci *98*, skaa122.

27. Song, C., Yang, J., Jiang, R., Yang, Z., Li, H., Huang, Y., Lan, X., Lei, C., Ma, Y., Qi, X., and Chen, H. (2019). miR-148a-3p regulates proliferation and apoptosis of bovine muscle cells by targeting KLF6. J. Cell. Physiol. *234*, 15742–15750.

OMTN, Volume 22

Supplemental Information

circFLT1 and lncCCPG1 Sponges miR-93 to Regulate the Proliferation and Differentiation of Adipocytes by Promoting lncSLC30A9 Expression

Zihong Kang, Sihuang Zhang, Enhui Jiang, Xinyu Wang, Zhen Wang, Hong Chen, and Xianyong Lan

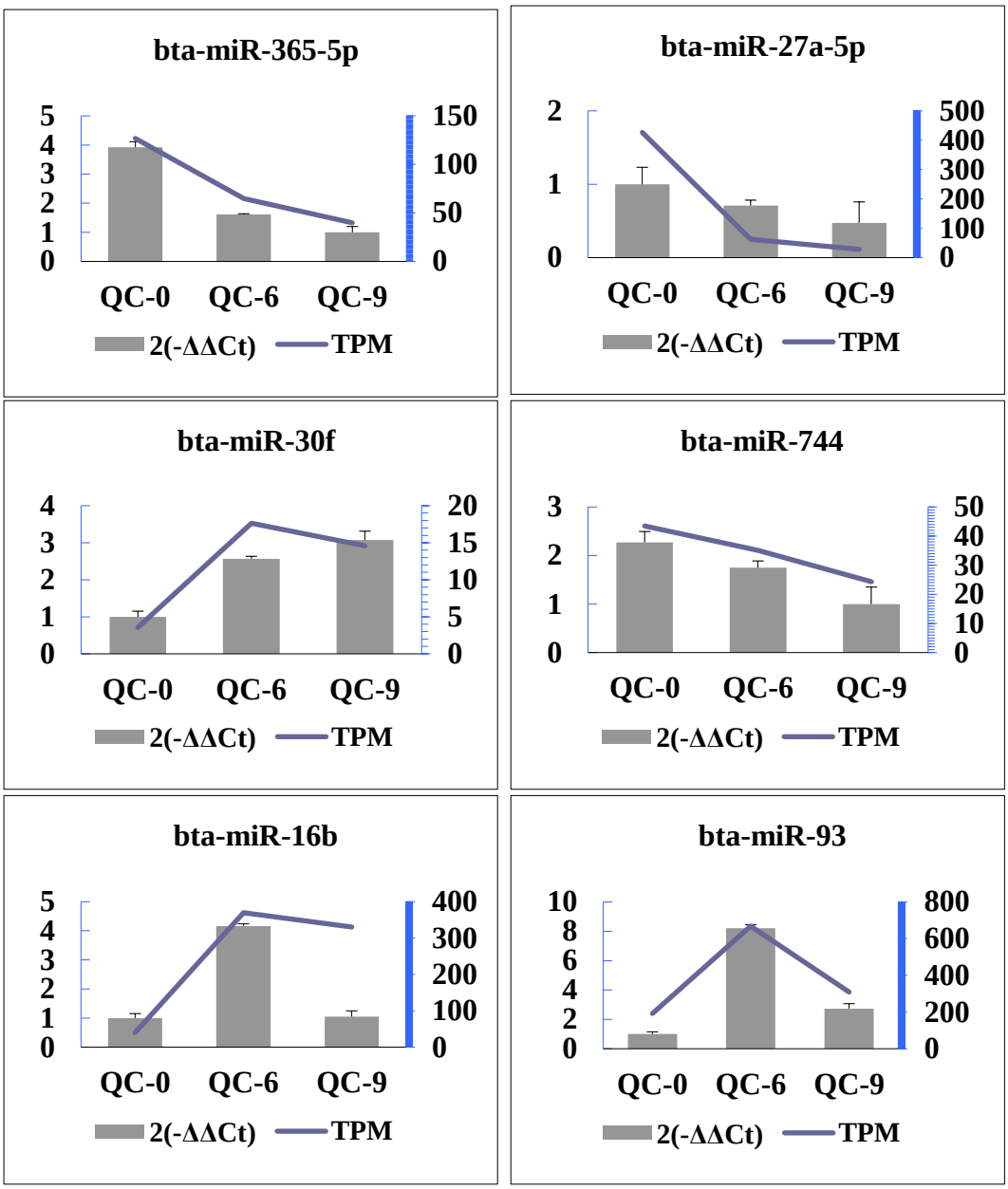

Supplementary Figure 1. RT-qPCR verified the sequencing results.

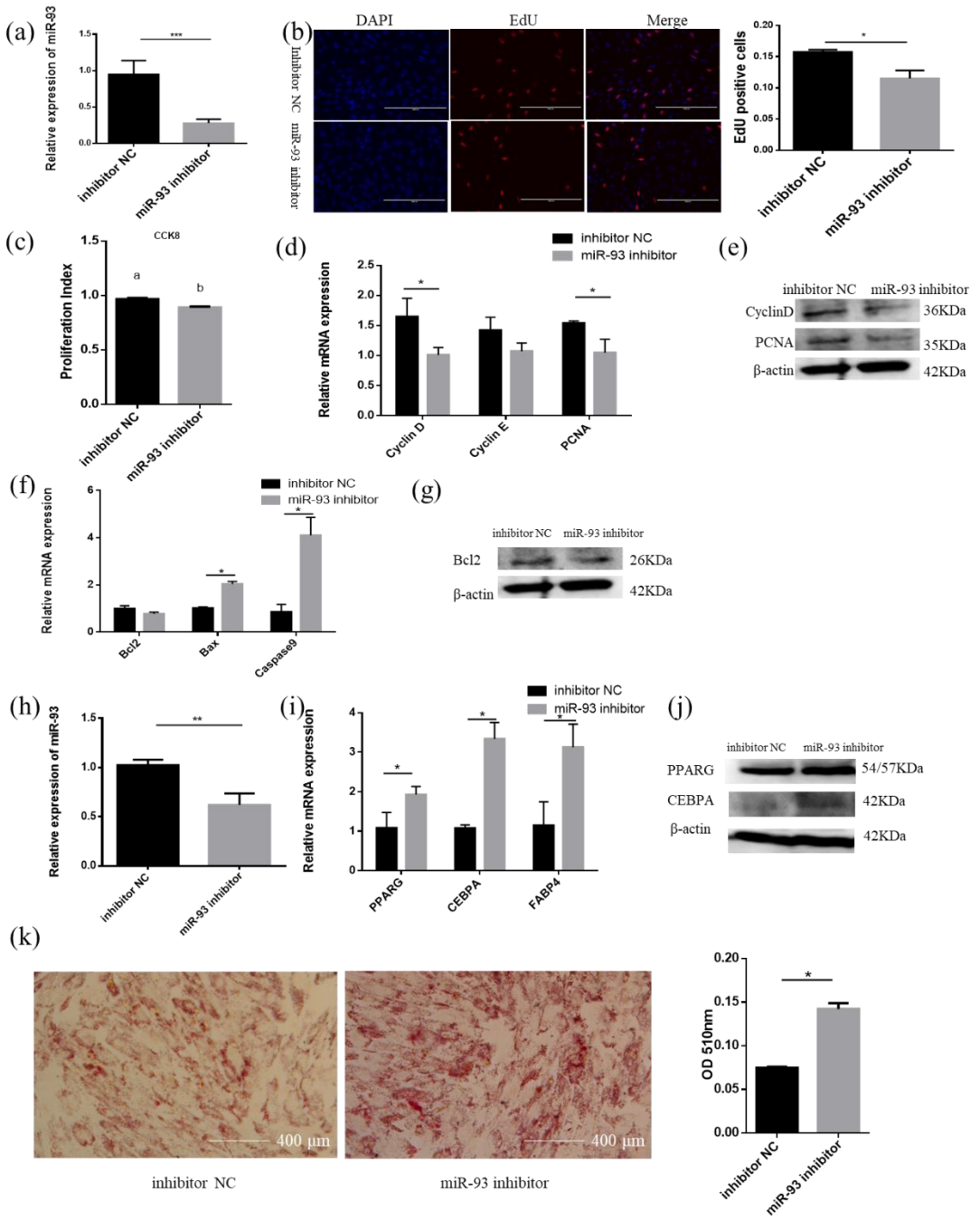

Supplementary Figure 2. Effect of miR-93 on proliferation, apoptosis, and differentiation of adipocytes. (a) Know down efficiency of miR-93; (b) Cell proliferation was measured with 5-ethynyl-20-deoxyuridine (EdU); (c) Cell proliferation index was measured by cell counting kit-8 (CCK-8) assay; (d)(e) The expression of proliferation marker genes were measured by real-time qPCR and western blotting. (f)(g) The expression of apoptosis marker genes were measured by real-time qPCR and western blotting. (h) Know down efficiency of miR-93;(i,j) The mRNA and protein expression of cell differentiation markers were measured by real-time qPCR and western blotting. (k) Oil red O staining was used to detect the production of lipid droplet. Values are mean ± SEM for three biological replicates, the different letters (a, b) means $P < 0.05$; *$P < 0.05$; **$P < 0.01$; ***$P < 0.01$.

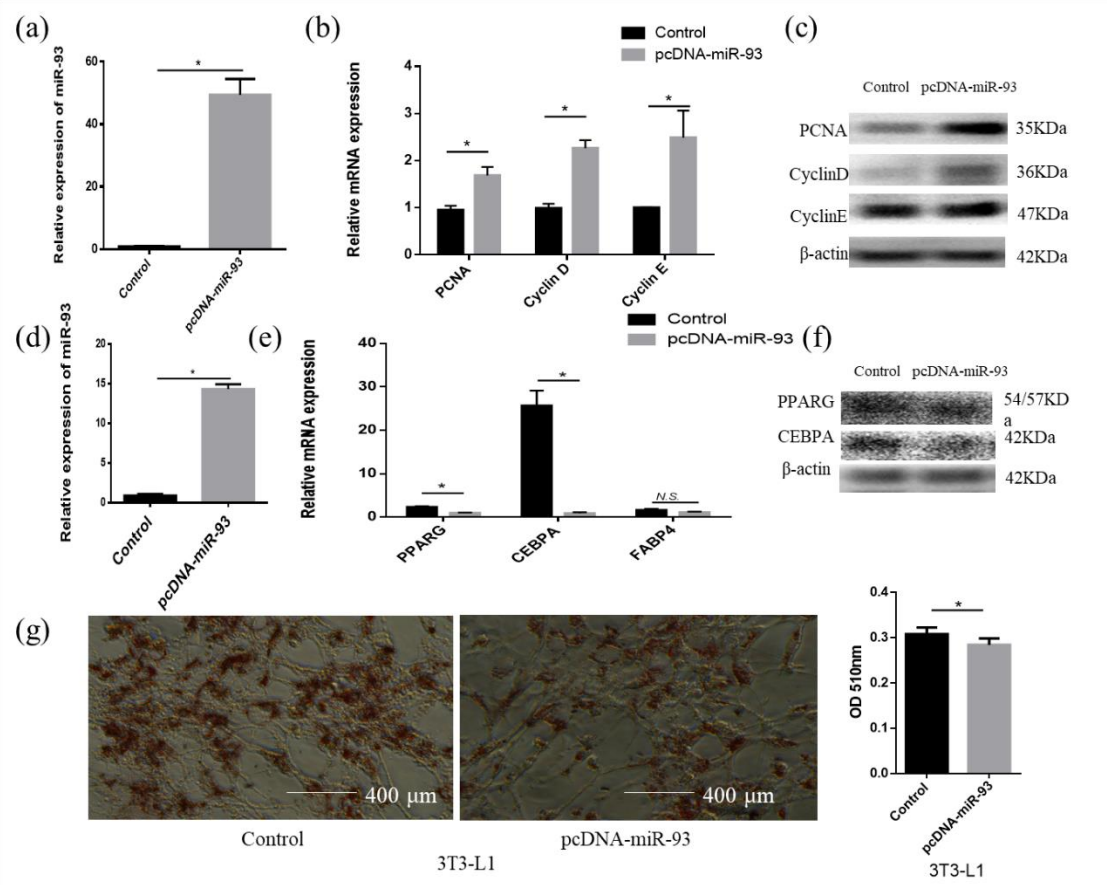

Supplementary Figure 3. Effect of miR-93 overexpression on 3T3-L1 cell proliferation and differentiation. (a) Overexpression efficiency of miR-93. (b,c) Expression of the proliferation marker genes were measured with real-time qPCR and western blotting. (d) Overexpression efficiency of miR-93. (e,f) The mRNA and protein expression of cell differentiation markers were measured with real-time qPCR and western blotting. (g) Oil Red O staining was used to detect the production of lipid droplet. Values are presented as mean ± SEM for three biological replicates, $*P < 0.05$.

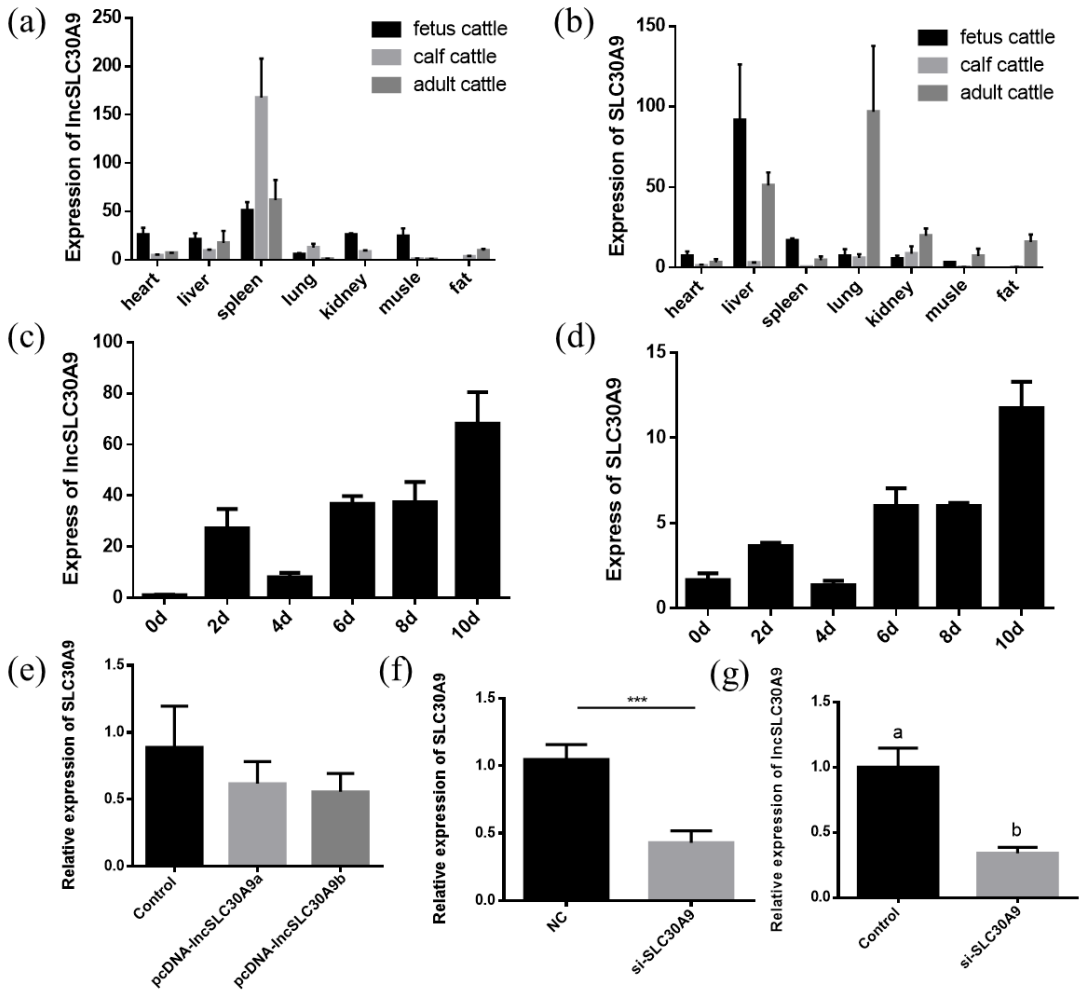

Supplementary Figure 4. Expression pattern of lncSLC30A9 and its maternal gene SLC30A9. (a) LncSLC30A9 tissue expression profile. (b) SLC30A9 tissue expression profile. (c) LncSLC30A9 was expressed at different time series. (d) SLC30A9 was expressed at different time series. (e) The influence of lncSLC30A9 on the expression of SLC30A9. (f) Know down efficiency of SLC30A9. (g) The influence of SLC30A9 on the expression of lncSLC30A9. Values are presented as mean ± SEM for three biological replicates. Different letters (a, b) indicate significant differences $P < 0.05$; ****$P < 0.001$*.

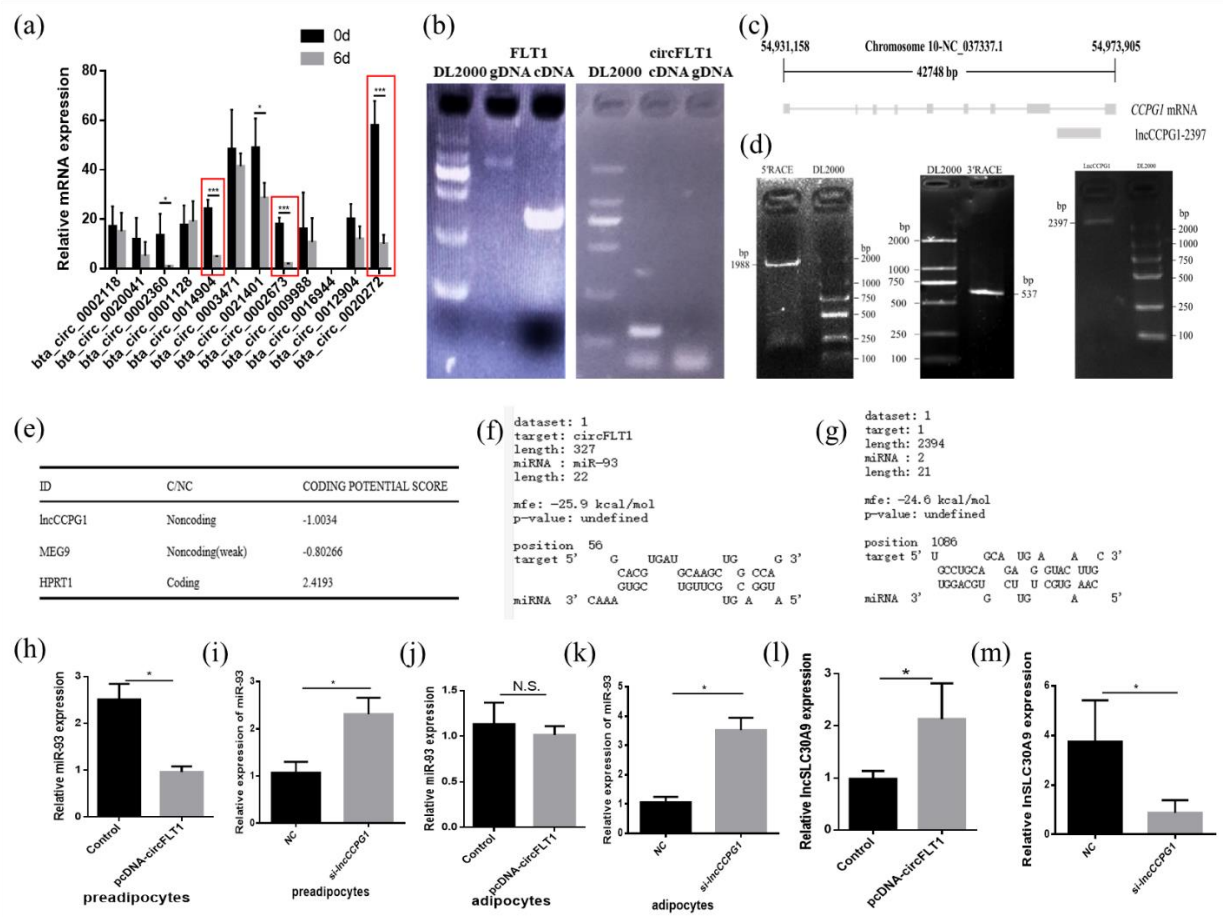

Supplementary Figure 5. circFLT1 and lncCCPG1 identification and interaction analysis. (a) circFLT1 screening. (b) Authenticity of circFLT1 verification. (c) Genomic structures of lncCCPG1. (d) The 5'RACE and 3'RACE analyses demonstrated the full length of lncCCPG1. (e) The RNA sequences of lncCCPG1 were processed by the Coding Potential Calculator (CPC) program and were predicted to be non-coding RNAs. (f,g) The RNAhybrid tool predicted the miR-93 binding sites at one distinct position in circFLT1 and lncCCPG1. (h-k) circFLT1 overexpression or lncCCPG1 knockdown effect the relative abundance of miR-93. (l,m) circFLT1 overexpression or lncCCPG1 knockdown effect the relative abundance of lncSLC30A9. Values are presented as mean ± SEM for three biological replicates, *$P < 0.05$; ***$P < 0.001$.

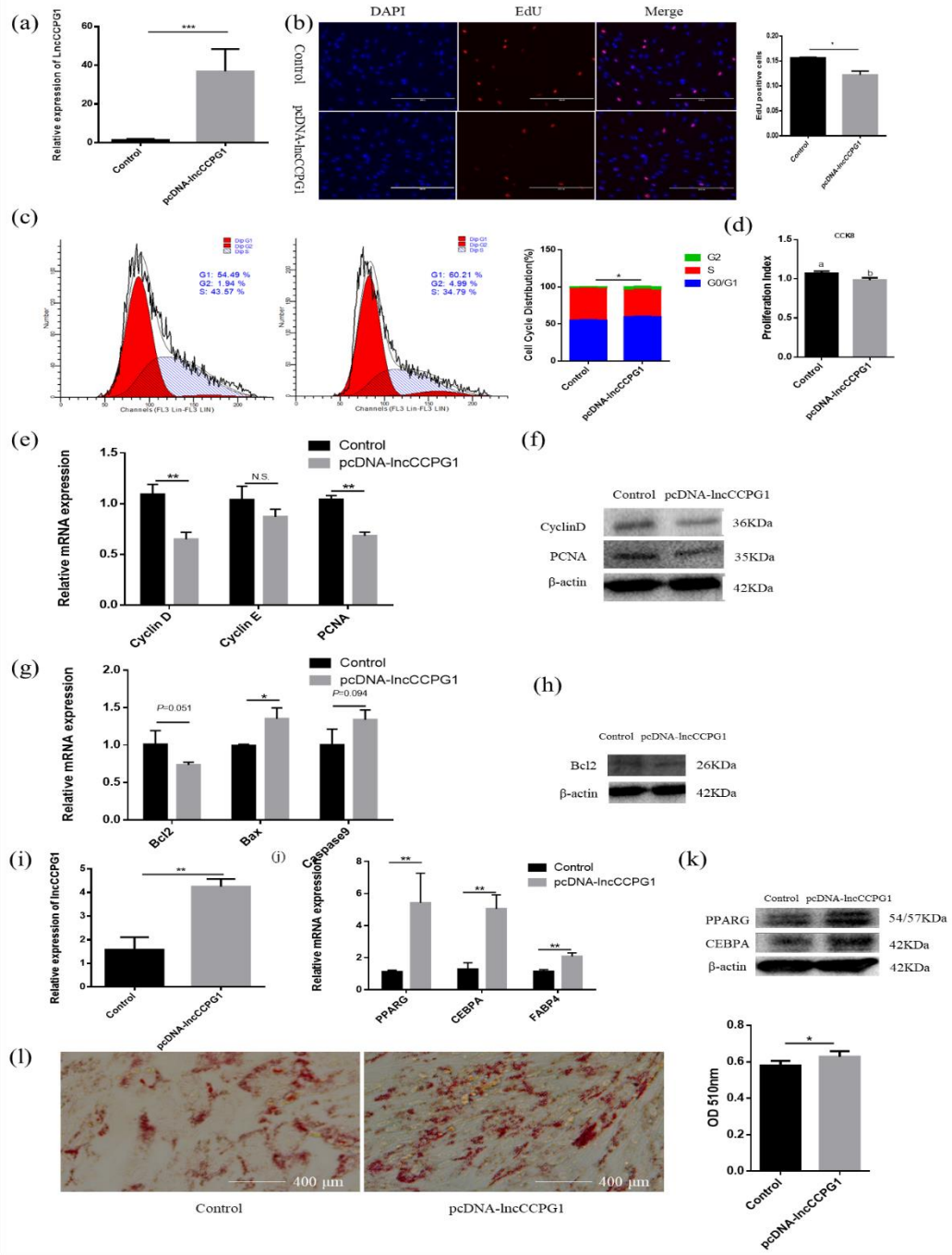

Supplementary Figure 6. Effect of lncCCPG1 on proliferation, apoptosis, and differentiation of adipocytes. (a) Overexpression efficiency of lncCCPG1; (b) Cell proliferation was measured with 5-ethynyl-20-deoxyuridine (EdU); (c) cell phase analyzed by flow cytometry; (d) Cell proliferation index was measured by cell counting kit-8 (CCK-8) assay; (e,f) The expression of proliferation marker genes were measured by real-time qPCR and western blotting. (g,h) The expression of apoptosis marker genes were measured by real-time qPCR and western blotting. (i) Overexpression efficiency of lncCCPG1; (j,k) The mRNA and protein expression of cell differentiation markers were measured by real-time qPCR and western blotting. (l) Oil red O staining was used to detect the production of lipid droplet. Values are mean ± SEM for three biological replicates, the different letters (a, b) means $P < 0.05$; *$P < 0.05$; **$P < 0.01$.

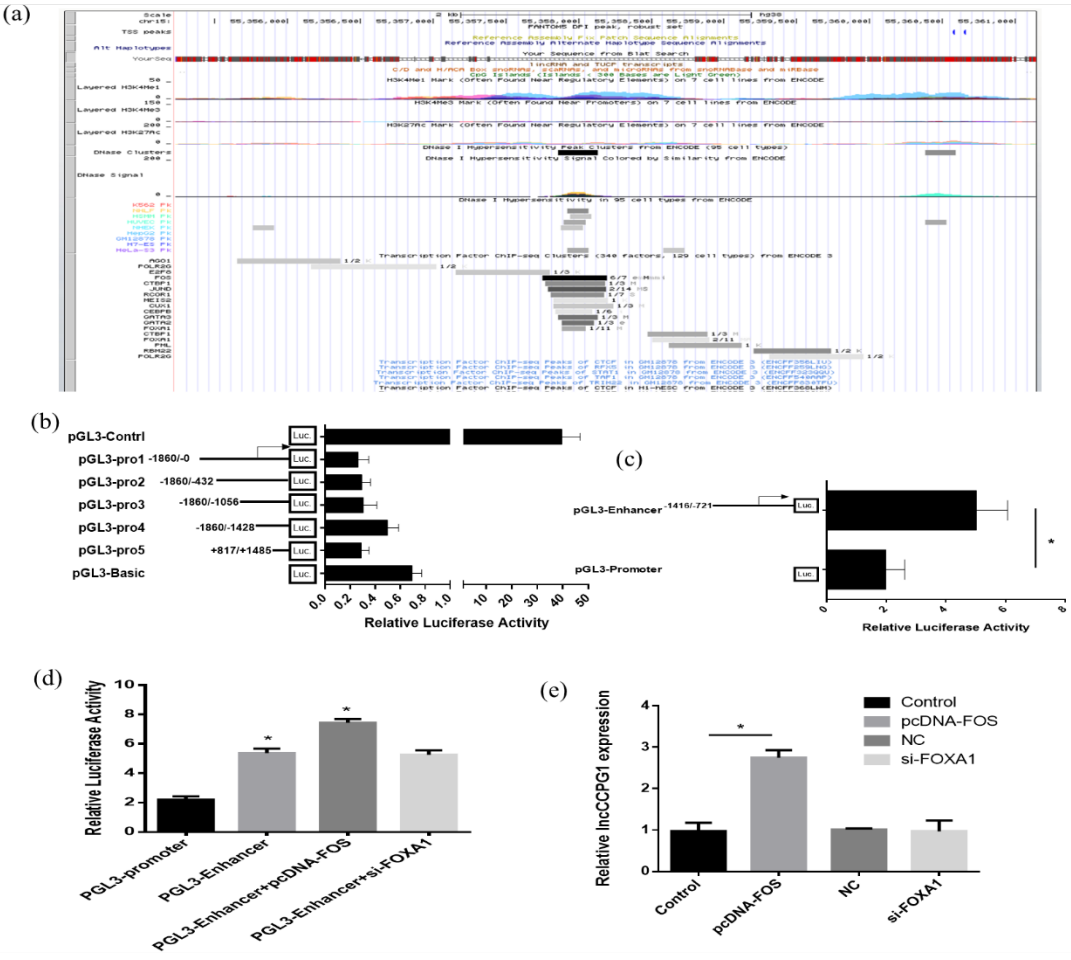

Supplementary Figure 7. Fluorescence activity analysis and transcription factor validation. (a) Sequence analysis by UCSC. (b) Promoter activity analysis. (c) Enhancer activity analysis. (d) Effects of overexpression of FOS and knock down of FOXA1 on enhancer activity. (e) Effects of overexpression of FOS and knockdown of FOXA1 on expression of lncCCPG1. Values are mean ± SEM for three biological replicates, $*P < 0.05$.

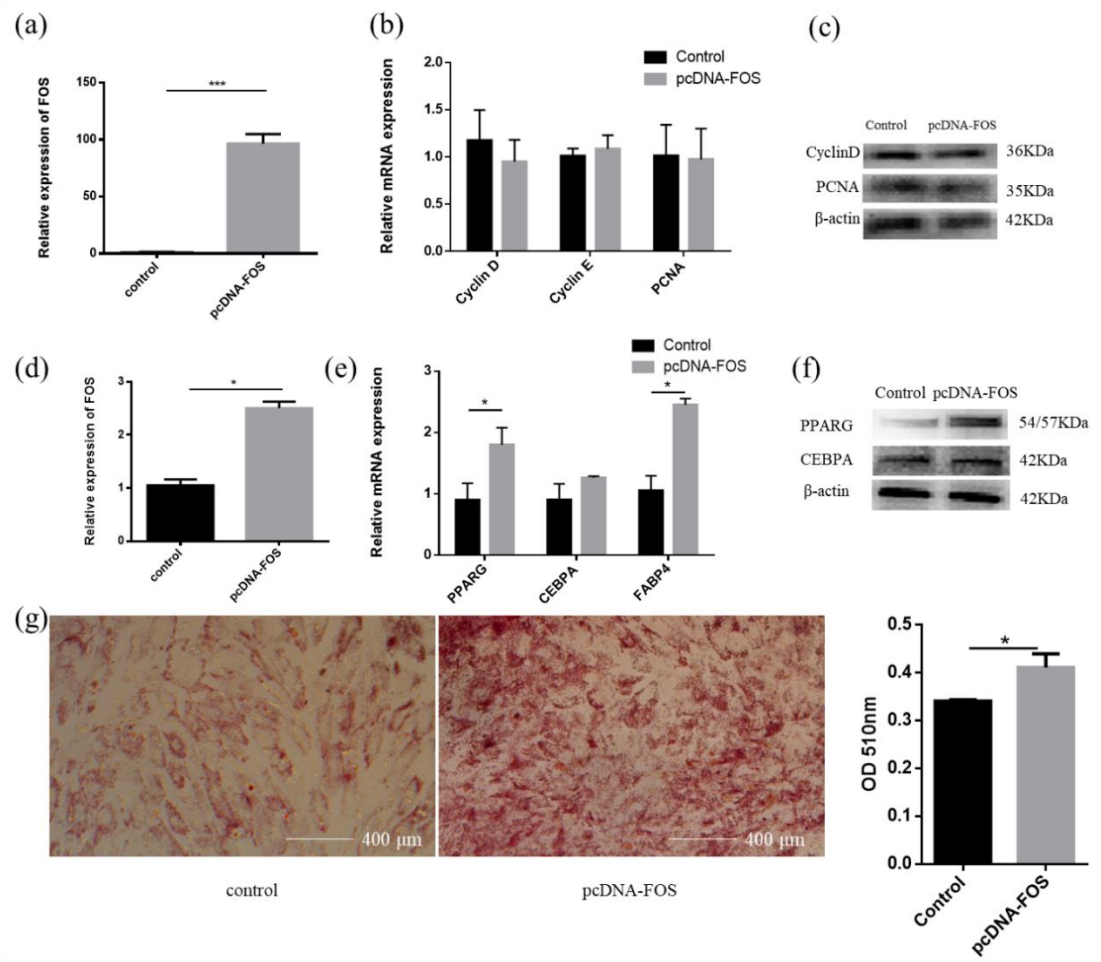

Supplementary Figure 8. Effect of *FOS* on proliferation and differentiation of adipocytes. (a) Overexpression efficiency of *FOS*; (b) (c) The expression of proliferation marker genes were measured by real-time qPCR and western blotting. (d) Overexpression efficiency of *FOS*; (e,f) The mRNA and protein expression of cell differentiation markers were measured by real-time qPCR and western blotting. (g) Oil red O staining was used to detect the production of lipid droplet. Values are mean ± SEM for three biological replicates, $*P < 0.05$; $***P < 0.001$.

Supplementary Table 1. Primers sequence for PCR and qRT-PCR
(submitted as a separate file)

Supplementary Table 2. The primary antibody and secondary antibody

Antibody name	**Purpose**	**Source**	**Catalogue Number**
Actin	primary antibody	Abbkine	WL01372
PPARG	primary antibody	Wanleibio	WL01800
CEBPA	primary antibody	Wanleibio	WL01899
PCNA	primary antibody	Wanleibio	WL02809
CyclinD1	primary antibody	Wanleibio	WL01435a
CyclinE	primary antibody	Wanleibio	WL01072
Bcl-2	primary antibody	Wanleibio	WL01556
AKT	primary antibody	Wanleibio	WL0003b
pAKT	primary antibody	Wanleibio	WLP001a
Goat Anti-Rabbit	secondary antibody	BOSTER	BA1041

LncRNA and circRNA sequence information

Lnc30A9a-1296nt

CTAGAGACCTTTATGCTTAAACATGGAGAAAATATTATTGATACTTTAGGAGCTGAAGTA
GATAGACTTGAGAAGGAACTGAAAAAACGAAATCCTGAAGTTCGACATGTAGATTTAGAG
ATATTATAAACTTGATGGGATGAATCACCTTGGAGGGAGCCTTGGAACCAAGTTTGCCAA
GACTACTTTCCCACCCTGAGGGAGTCAATGCCATTCAGAAGCCGTTTATTTGAAGATGGAG
GAAGTATTTATATGAAAAGGGCAATTCAACAGTCCATAGAACTAAAACAGCTTCTTCTAA
GAGACCTATTACAAGTTGAATCAATTTGGAAATCATGTTTTTATGTTTCAATGGAAACGTT
TTAGTTACTTAAATTGTTCATAATTTCTTACTTTAGCCTGTCAGTGTGTATTGTACCTGCAA
TCATGTTTCCTTCCTTCACATGGGTAAAAATAAGCAGCATCCGTAAGATTATGATTTTTTAT
TTTGTGGCCAGTGAAGATTTCACTCCATCAAAACCTGTCAATCTTGAACATTCTGGCTAAA
TCTTGTATTCTGGTTTTTGAAACAGTCACTCCATTTTCAAAGTCTGTCTTTCCTTACAGAAT
GTAGAAATTATTTTGACATAGGTTGTCAAACCTGAGCACTAAGAGGAACACTGTCGTAAT
AACTTGGTTATCCATAAATGTTCATTCCAATAGGACTCTGTTACTGAATTGAAGGAAGATA
ACTTCAGTACACTCTTTTAGGTCATGCTAGTTGCCATTTTGTAAAATTTCTTTTCTCTCCTTT
GTTTTTTTCCTTATTTAGTTTAATTTTTCTAATGGTAGGAAATATAAAATAACCCTAGATGT
TTCCATGGGCCAGTGTGATGACTGGTTTTTAGTTTTTGTTTTTTTTTAACTGGCTCCAATGCT
GCCATGTGTATTTACTAGGAGATAATGCATTTATAAGTATTTTAACATTCTGTAAAGTGGA
CTAGAAATATTTATAATTTTACAGACACCACAGCATTTTATTTTTAATTTATTTTAAAAGAG
GCACTACTTATGTAAATCTGAACTGTGTGATATTTCTTGCTTTAAGAGATAGAGACATAAA
CCTCTTATACAAAAACTTGTGACCATGACTTTGTTTAATATCATAGTCAATAGTGTAACAT
GAGTTTCTTGCAGTTACAAATGGGCATTTAGCATAAAGTATGATTATAAATTATGTAAGTA
GCTTTCTGATGATCATAAAGTATCAAGGTGAAAAAACATAATTCAGTAATTAAAAACTGA
GTGCAAAACTACA

Lnc30A9b-848nt

TAAAAATAAGCAGCATCCGTAAGATTATGATTTTTTATTTTGTGGCCAGTGAAGATTTCAC
TCCATCAAAACCTGTCAATCTTGAACATTCTGGCTAAATCTTGTATTCTGGTTTTTGAAACA
GTCACTCCATTTTCAAAGTCTGTCTTTCCTTACAGAATGTAGAAATTATTTTGACATAGGTT
GTCAAACCTGAGCACTAAGAGGAACACTGTCGTAATAACTTGGTTATCCATAAATGTTCAT
TCCAATAGGACTCTGTTACTGAATTGAAGGAAGATAACTTCAGTACACTCTTTTAGGTCAT
GCTAGTTGCCATTTTGTAAAATTTCTTTTCTCTCCTTTGTTTTTTTCCTTATTTAGTTTAATTT
TTCTAATGGTAGGAAATATAAAATAACCCTAGATGTTTCCATGGGCCAGTGTGATGACTG
GTTTTTAGTTTTTGTTTTTTTTTAACTGGCTCCAATGCTGCCATGTGTATTTACTAGGAGATA
ATGCATTTATAAGTATTTTAACATTCTGTAAAGTGGACTAGAAATATTTATAATTTTACAG
ACACCACAGCATTTTATTTTTAATTTATTTTAAAAGAGGCACTACTTATGTAAATCTGAAC
TGTGTGATATTTCTTGCTTTAAGAGATAGAGACATAAACCTCTTATACAAAAACTTGTGAC
CATGACTTTGTTTAATATCATAGTCAATAGTGTAACATGAGTTTCTTGCAGTTACAAATGG
GCATTTAGCATAAAGTATGATTATAAATTATGTAAGTAGCTTTCTGATGATCATAAAGTAT
CAAGGTGAAAAAACATAATTCAGTAATTAAAAACTGAGTGCAAAACTACA

LncCCPG1-2397nt

GGGGGGTTAGTCTGCATATGACCTATGGTCAGCCCTCTGTATCAGCATTTCTGCATCTGAG
GATTCAACCAGCCACAGACCATGTAGTACTGAAGTATTTACTATTGAAAGATATCCAGGT
ATAAATAGACCCAAGCAGTGCAAACCCACATTGTTCAAGGGTCAGCTGTATTTGTTGTAA
AAGTACTTTTTGTAAACAAAAGTACTATTTGTAAAAGTATTTTATTGCCTTGGAATTCAGG

ATAAATTGAAAGATTAAATTTTAAGTTAAAATCTATTACAAACTGAAAATTTCATAAAATC
AGTTTGACTTGAGCAAATGGTTTAATTTCTACCTTAAAAAATCTGAGGATATAAAATTCTA
TTTTAGCCTATTTCATTTTTTTCATTATACTTTATATGAAAAGATAATCACCTTAAGTTATTT
CCTTAATCTTTTATTTACTCACTCAACTCTGGGAAGCTAGGAGTGAAAAATACAAATTTCA
CTTTGAAATCAGAGTAACAATTCAAGTGTCCCACTTGCTTTGTCTATTCTACTTACCAACTA
AATTATGATATTTAATACATTTATTATAGAATTATTATTGGTAGAGGCATGATCAAAGGGG
TAAACTTTGCAAGCCACAAGTTCTCATGCGTGTGCTTTATATATAACCTTTAAAAATAACA
TTGTATTATCCATTGCTTACCAGCTTTCTATTCTGTAACACAAAACTCTCCTAATCTTTGAA
TGTTAGCTTTATTTTTTAACCTTTGAGATATTTTTCTCTATATAGCTTTTTGAATAAACGTA
ATGTGTCAATAAAATAATGAGACTGATTTTGGTGTCTTTAGTCATTAAATACATATCTAGA
GCAAAGTACTGTGAGGCTGTCCTGAGGAAAGAAATGAAAAATTCTTGCTGTCAAGGAGCT
CAGAAGCTTTTGGAGAATTAGGTCAATACAAGAAATGCAGTGGAGATGTGGAGGCATATT
ATATGCTGGCCTCAGTCAACAGATGTTTGGGAAGGCTTCATAATAAGATGGCCTTTGAGCT
GAACTTCTTTTTAACTGGTTTTTGAAGAAGTAGTGAAAACTTGCCTGCAGCAGATGGAGTA
CATTGCACTCAAAGGGAACTTCATTTGCACTGATTTGGAGATGTGAAGACATGCTGTGTTA
AGGAGACAAGGTAGAGGTGGGGGGTAAACAGAAGAAAAGATTCAGATCATGAAGAACTT
TTATGCTGGAGGACTTGTTTTATTGCATTTTGGGTCACTGGCAGCAGCCTGAAGGGTTTAT
TGGAAAGAGTGAAGCTAGATGCTGAAAAGTGGTTTTTGAAATGATACAGACATGAGCTGA
TGAGTATCTGAACTAGGGCAGTAGCAGGAATAGAAAGGAGGGGACAGATTTGAACGGTA
TATAGTAAGTAAAATCGGTGCTATTTCTTGTGAAATAGAAGTAGAAAGTAACAATGCCTTT
TGAGATTTCTGGGTTGGGTCACTAGTTATATAGTTACATATATATGTCTATAGTTATAGGT
GTGTGTGTATATATATGTATATTCTATATATATATAACTGTTTAGTTATATATGGACATTAG
CTACACTAAGGAATACCAGGGCTTGGGTGAGGGGAATTGAAAATGAGAATTGTGGTTGGT
ATTTATTGACATAAGTAGGGAGAATTTGTTGGCCATTAGTTATGTGACTCTGTCTCTAGTC
CAGACTCTGTATATGTAGATAGTCTAGGCTGGAGGTGTTTATCAGACTCCTGAAGAACACC
AACATCTAAGGGATTGTAGAGAAAGAAGGCTGAGAATGAATGATGGGCAGAGAGTGGCA
TTGTGAAAATCGAAAATCATCTCAAGTAAAAGGAATAATGTTACATGCTGCCCCCCCGCC
CCCCAAAAAAAGAATGGATGTCTTGGTTGGGAATTGGACGGCCATGGAGTGTTTTGTTGA
AGTAGTGACAAAGGTGTGATTATGGAGATCAAGAACTACATGTAGATATTGTTTATAAGC
CTTAGCTGTTAGAGCATGCATGCGCATGCAGAAAAGAGGGAGGGAGGGAGGAACTCTGTT
GGAACTGTGTATGTATCCCTGCTGAGGGAGGAAGCCACTTGGGGAGGGGGAATTAATTTT
AATAGGAAAGGAGAAAAAATAATGGAAACACATCTCATTATTTTATTGTCACATTTCTATT
TATCTTTTGAGTGTTTCCCCTGTTTGCCAGCACAGTTATGTTTGTCCATTTTTTCTTTCTGTA
GGATAAAAGTATAAACTCACTGAAATCTTTTTTATATGGTTATACTAGGATTATATACTTC
AGATTCATTTACTATCCTTTTTCAGTGTTCAGATAATAGATTAATGGAGAAAAAACATTAA
AATTGTTTCTTGTTTAAATA

FLT1-327nt

GATCTAGTTCAGGTTCAATATTAAGACATCCTGAACTGAGTTTAAAAGGCACCCGGCACGTG
ATGCAAGCTGGCCAGACGCTGAATCTCAAATGCAGAGGAGGAGCTGCCCATGCCTGGTATC
TGCCTGAAGCTGTGAACAGGGAAAACCAAAGCGGGAAGCTTAACATCACTAAGTCTGCCT
GTGGAAAGAACCTCAAGAAATTCTGCAGCACTTTGACCTTGAACGCGGCTCAGGCCAACC
ACACTGGCTTCTATAGCTGCAGATATCTCTCTGCACCTGCTTCCAAGAACAAAGCAGAATCT
ACCATCTACATATTTATTAATG

Note: Red represents the joint sequence